Regional Rice Yield Forecasting Using Landsat 8 Satellite Imagery and DSSAT-CSM

By

Saima Iftikhar

(NUST201463294MSCEE62514F)

A thesis submitted in partial fulfillment of the requirements for the degree of Master of Science in Remote Sensing and GIS

Institute of Geographical Information Systems
School of Civil and Environmental Engineering
National University of Sciences & Technology
Islamabad, Pakistan

December 2016

CERTIFICATE

ACADEMIC THESIS: DECLARATION OF AUTHORSHIP

DEDICATION

Dedicated to my Family, especially to my Baba Jan

AKNOWLEDGMENT

I bow my head before God Almighty for helping me complete the challenging task of undertaking an interdisciplinary research project that required extensive data acquisition and its application using multiple approaches and supportive technologies. May the blessing of Allah be upon the Prophet Muhammad (peace be upon him), who mandated every Muslim man and woman to acquire knowledge and become dynamic member of the society.

I value and cherish the research environment provided by my University (NUST) and within that the School of Civil and Environmental Engineering (SCEE). I appreciate the guidance provided by the faculty of Institute of Geographic Information Systems (IGIS) and in particular the advice and support given by my supervisor and HOD Dr. Javed Iqbal. I express my gratitude to Dr. Ijaz Hussain, Associate Dean (IGIS), my co supervisor Dr. Ashfaq Ahmad Chattha (UAF), Dr. Mukhtar Ahmad (PMAS) and Mr. Junaid Aziz (IGIS).

I gratefully acknowledge the support provided by Pakistan Metrological Department (PMD) in giving thirty years of climatic data of Sheikhupura District, Soil Survey of Pakistan for providing the basic data on the soil characteristics of Sheikhupura, Ayub Agriculture Research Institute with its subordinate institute, Rice Research Institute of Kala Shah Kaku for the data on PS2 cultivar. I also thank University of Agriculture Faisalabad for providing technical data used in DSSAT-CSM. I am especially indebted to Dr Mukhtar for helping me understand the concept and functioning of DSSAT-CSM.

To my baba, I thank you for always being there for me, enabling me to be who I am and where I am today. You have been the constant source of love, support and encouragement, which makes everything possible.

Table of Contents

List of Tables

List of Figures

List of Appendices

List of Abbreviations

Abbreviation	Definition
CEC	Cation Exchange Capacity
CI	Change Index
CO_2	Carbon Dioxide
CSM	Crop Simulation Model
DSSAT	Decision Support System for Agrotechnology Transfer
EM	Electromagnetic
EVI	Enhanced Vegetation Index
FAO	Food and Agriculture Organization Of The United Nations
FP	Four Pixels
GDP	Gross Domestic Production
GIS	Geographic Information System
GPS	Global Positioning System
GOBPC	Geographic Information System Base Post Classification
IBSNAT	International Benchmark Sites Network for Agrotechnology Transf
ICT	Information and Communication Technology
IPPCC	Inter-governmental Panel on Climate Change
KSKRRI	Kala Shah Kaku Rice Research Institute
LAI	Leaf Area Index
MDS	Minimum Data Sets
NIR	Near Infra-Red
NP	Nine Pixels
PAR	Photosynthetically Active Radiation
PMD	Pakistan Metrological Department
RS	Remote Sensing
RVI	Ratio Vegetation Index
SUPARCO	Space and Upper Atmosphere Research Commission
VI	Vegetation Index

ABSTRACT

Rice (Oryza sativa L.) is the second main food crop after wheat in Pakistan and a key source of export earnings. To ensure food security, timely and accurate estimation of micro/macro level estimation of crop yield is important. A study was conducted in district Sheikhupura, a major rice growing area of Pakistan, with the objective to use remote sensing and crop model for rice crop yield estimation. The results of these two techniques were validated with field survey data. Landsat 8 satellite imageries were downloaded covering different stages of rice crop growth (July to November 2015). Satellite data was pre-processed in ENVI software. Normalized Difference Vegetation Index (NDVI) of rice crop was calculated for all the six imageries (n=33) of the growing season and correlated with observed yield. The highest relationship (R^2=0.788; $p \leq 0.05$) between NDVI and observed yield was recorded on September 29, 2015. The NDVI map of September 29, 2015 was used to generate rice yield map using a linear regression model. A best fit was found between observed and NDVI calculated yield (R^2= 0.738; RMSE=178 $kgha^{-1}$). The raster map of the crop yield was used for computing the total crop production of the entire district. A comparison of the calculated production and area under rice cultivation with those of the Crop Reporting Survey of Punjab found to be 14.6 % and 9% higher, respectively. The Decision Support System for Agrotechnology Transfer (DSSAT)-Crop Simulation Model (CSM) was also used for prediction of the final rice yield based on farmers' field inputs and other data i.e. climate, soils and genetic coefficients of the selected crop etc. A best fit was found between observed and DSSAT predicted yield (R^2= 0.928; RMSE=111 $kgha^{-1}$). The results of the study showed that the DSSAT predicted the rice grain yield more accurately than the RS technique. However, DSSAT-CSM needs extensive data input and has constraints of spatial extrapolation.

Chapter 1

INTRODUCTION

1.1 Background

Pakistan is a developing country with agriculture sector as a vital component of its economy. Agriculture sector provides employment to 43.5 % of its population and contributes 20.9 % to its GDP, besides providing raw materials to agro-based industry. It is by far the largest consumer of water and a major consumer of energy. It plays key role in insuring food security for the nation (Pakistan Ecnomic Survey, 2014-15). Hence, agriculture sector lies at the heart of any study, research or policy formulation regarding energy, water and food security. Traditional methods, management practices, and technology application for improving agriculture growth have reached a stage of near stagnation. However, state of the art technologies are now available commercially and are being used worldwide to improve management practices of not only the production of crops but also the re food supply chain and its share in the broader one health concept. Nevertheless, before the policy makers and the farmers develop confidence in modern technology and knowledge inputs, they have to be shown the validity and reliability of these technologies, especially Remote Sensing (RS) and Crop Simulation Models (CSM). Accurate yield forecasting of major crops, especially wheat and rice, using new technologies like GIS and RS will give confidence to the policy makers in the validity as well as reliability of RS-based techniques. Accurate forecasting of rice yield therefore has a socio-economic and technological context out of which flow the objectives and research question of the study. While this research focuses primarily on the technological context, the socio-economic context will influence the choice of farmers for adopting new technologies, especially Precision Agriculture (PA).

1.2 The Socio-Economic Context

Pakistan is a heavily populated country that faces the challenges of water and food security. By 2050, Pakistan will be required to feed a population of 344 million (Ministry of planning, Development and Reform Islamabad., 2013). Pakistan Vision 2025 lays special emphasis on food security and seeks to protect the most food-insecure people by creating a diversified and efficient agriculture sector. Agriculture sector also feeds textile, food processing and other associated industries, that have a major share in exports too (Pakistan Economic Survey 2015-16). Wheat, rice, cotton and sugarcane together contribute 5.3% to the country's Gross Domestic Production (GDP). Rice is the second largest staple food (Khush, 2005) as well as a major source of export earnings. Almost all the countries and particularly those in the tropical and subtropical regions consume rice. However, in 2010, almost 88% of the World's total production of rice was grown in Asia that supports 60% of the World's population (GeoHive., 2010).

Pakistan ranks 11th in production and 5th in the export of rice in the world. About 0.7% of country's GDP comes from rice. The rice export earnings in 2014-15 (July-March) were about USD 1.53 billion. Rice recorded highest ever production at 7.0 million tons, showing a growth of 3.0 percent over corresponding period of last year's production. The increase in production was due to greater area under cultivation, availability of irrigation water and high yielding hybrid rice varieties (Pakistan Economic Survey 2014-15).

The 11th Five Year Plan 2013-18 has laid down the production targets for rice as 7.371 million tons by 2017-18 thereby expecting an increase of 1.87 million tons from the benchmark of 5.5 million tons in 2012-13. It may be added here that rice production back in 2008-09 was actually 7 million tons and therefore achieving the target of 7.371 million tons in 2018 is not an impossibility(11th Five Year Plan 2013-18 Planning commission, Ministry of planning, Development and Reform Islamabad, 2013). However, it must be kept in mind that Pakistan is water stressed country today and is likely to be water scarce country in future (Brisco, 2005). It will ultimately affect the production of rice, which is the biggest user of water among other crops.

Production of rice is not limited to the farm practices and other soil and metrological factors but to the socio-economic and political aspects of the area under cultivation. The rice production system in Punjab Pakistan reveals that the price structure of rice discriminates against growing rice by negative private profitability and lack competitiveness at the farm level in Punjab, Pakistan. It expresses the need for removing distortions in policies to give more incentives to the growers (Akhtar et al., 2007). Agriculture sector is in dire need of research on its social and economic aspects than in the pure scientific research by agriculture universities and research councils (Amjad, 2010).

1.3 Technological context

In the recent times, climate change and population growth, especially in major rice growing and consuming countries, have put a lot of pressure on demand and production of food in the world (GeoHive, 2010; IPCC, 2014; Wheeler & von Braun, 2013). Food security in many areas of world is expected to be major issue especially in the populous countries that are also heavy consumers of rice (IPCC, 2014). Hence, early forecasting of rice production using reliable technological means and method will be important. In order to offset food shortage, governments and economic managers look for reliable tools for early and timely estimation and forecasting of rice production. They have to formulate appropriate policies to work out possible surpluses that will require export of rice to other countries and shortfalls requiring import to prevent food shortage in the country (Noureldin et al., 2013). Early information on likely reduction in the production of rice can also trigger early purchase of rice at lower prices by the government, while guarding information on likely shortfalls thereby preventing exploitation by the profiteers.

Thus Vision 2025 and 11th Five Year Plan; 2013-18 talk of improving total factor productivity and competitiveness of the agriculture production system through technology based intervention with emphases on small and medium size farmers and landless tenants. It calls for paradigm shift from resource-intensive to resource-conservation technologies for more productive, competitive and sustainable farming system. In other words precision agriculture is the solution to many such problems in agriculture sector (Ministry of Planning, Development and Reform Islamabad., 2013). Within precision agriculture technologies, GIS and RS play a very important role in providing the essential inputs for subsequent application of agriculture extension technologies. GIS and RS, computer modeling for individual crops provide an important technological tool to the decision makers who are interested in forecasting agricultural production and its marketing, storage and export potential (Kirthiga, 2013). GIS & RS have been used extensively for crop yield forecasting around the world but in Pakistan its application has not been combined with traditional crop yield forecasting methods including field verification, and CSM. Even in the developed countries CSM have recently been integrated with RS inputs and real time met data.

Ideally a combination of optical remote sensing-based forecasting method and microwave remote sensing-based forecasting method should be used to have more accurate yield forecasting under all kind of weather conditions(Mosleh, 2015). However where resource constraints deny microwave remote sensing means, one has to rely primarily on optical remote sensing means.

This study is therefore limited because of the availability of optical remote sensing imagery only. To make up for this limitation, an effort has been made to acquire requisite data through field survey and agro-technology modelling using DSSAT (Decision Support System for Agro-Technology Transfer). DSSAT modelling requires data on weather over an extended period, soil conditions, especially within the top layer that supports rice growth, authentic cultivar research data and field management data of specific crop. The results of DSSAT modelling have to be compared with those of GIS and RS.

1.4 Purpose of Study/Justification

Sheikhupura is an important area for rice production, as it contributes significantly to the national economy. Developed countries have done a lot of research on rice yield forecasting using state of the art technologies. However, many developing countries like Pakistan have not done it effectively. Current investigation would be of great value in introducing stat of the art technologies rice yield forecasting in Sheikhupura region. In season, forecasting of rice yield using Remote Sensing and CSM will help the policy makers estimate rice production much before the actual harvest for planning and determining likely deficiencies/surpluses that warrant measures to control consequent price fluctuations in the market. Likewise, possible surpluses would require timely action for exports.

1.5 Statement of the Problem

Rice yield assessment based on the field reporting and data collected by conventional methods is time consuming, subjective, costly and unreliable. It has contributed significantly towards discouraging introduction of new knowledge and technologies in formulating suitable policies concerning food security and improving on farm management practices. A more accurate and timely (in-season) crop yield forecasting using stat of the art technologies is thus a dire necessity. This study aims at combined application of RS and CSM approaches for accurate and reliable rice yield forecasting in Sheikhupura.

1.6 Distinctiveness of the study

This study uses the knowledge and technology of two domains of agri-sciences particularly DSSAT-CSM and RS & GIS technologies. The results of the two approaches have been verified by field survey/physical ground check. It is therefore an effort in inter-disciplinary research that will pave the way for further integrated application of knowledge and technologies.

1.7 Objectives

Following were the main objectives of the study:

1. To predict in season rice yield using satellite imagery and crop simulation model.
2. To validate the crop yield results of both methods with field survey data.

1.8 Research questions:

- With the available remote sensing data obtained from Landsat 8, how can we accurately forecast yield of rice?
- How accurate is the rice yield forecasted by DSSAT-CSM in comparison with the yield forecasted by RS and field data.

Chapter 2

LITERATURE REVIEW

2.1 Preamble

The application and use of technology in interdisciplinary domains is increasing with every passing year. Three factors are pushing the trans-disciplinary and inter-disciplinary boundaries using technologies like ICT and GIS & RS. The availability of the state of the art technologies in commercial markets at affordable prices. The application of precision technologies that have increased reliability and accuracy of outcomes. The system integration capability that is helping machines to handles complex problems. (Al-gaadi, 2010).

Use of drones for RS and GIS in crop management can now be combined with random checks through field surveys to calibrate simulation models and forecasting done by RS of large area by satellites. Agricultural production is significantly affected by environmental factors. Weather influences crop growth and development, causing large intra-seasonal yield variability. In addition, spatial variability of soil properties, interacting with weather conditions, cause spatial yield variability. Crop agronomic management (e.g. planting, fertilizer application, irrigation, tillage, and so on) can be used to offset the loss in yield due to the effect of weather. As a result, yield forecasting represents an important tool for optimizing crop yield and evaluating the crop-area insurance contracts (Basso et al., 2013).

In Pakistan, Crop yield forecasting has been done in the past using traditional methods most of the time. An improvement came in the form of simulated models that use metrological data, soil series data, cultivar data and crop management practices. However GIS and RS applications are now used quite frequently for yield forecasting specially for wheat (Ahmad et al., 2014). The primary role of GIS lies in bridging remote sensing derived information with the ground-based information and statistical data using several GIS-based techniques. Usually, GIS-based operations are performed for integration between ground data and remote sensing-derived information. These operations include: (a) generation of shape files; (b) addition of crop information to the attribute table of shape file; (c) overlaying the shape files on the remote sensing-derived surface, and extracting pixel-based information from remote sensing data; and (d) comparing the calculated data with the actual rice area and/or yield data. GIS and Remote sensing technologies are used as an integrated way in mapping rice area and forecasting its production. The literature reviewed in this study covers the application of GIS & RS method as well CSM based techniques and field survey for rice crop yield forecasting.

The literature under review falls in four categories:

- Judgmental forecasting.
- GIS and RS application for crop management
- Use of simulation models especially DSSAT-CSM for crop production forecasting.
- Combination of GIS & RS based approaches and simulation models application.

2.2 Judgmental Forecasting

Traditionally crop yield approximation in many countries was done using outcomes of agronomic research based on conventional experience, relying primarily on statistical analysis, while disregarding the underlying biological or physical principles involved. (Jame et al., 1996). Such a crop production approximation tends to be more subjective and is usually far from being timely and cost effective. This approach does not help in timely mitigation of impending food shortage and their negative impact (Sawasawa, 2003). A need has always been felt to undertake an in depth analysis of the factors affecting crop production and produce more accurate and timely results. Hence, different models for forecasting crop production are being developed in different countries**.** The main advantage of models thus developed would be to provide objective forecasts of regional yields in advance of the harvest proper, and at the fraction of the cost of sampling techniques. (Jame et al., 1996).

2.3 GIS and Remote Sensing Applications for Crop Management

The second approach in regional crop yield estimation is the application of Remote Sensing techniques to demarcate the cropped area spatially; to identify the present vigor of the crop by certain indices and relate it to final yield. This approach is considered an effective alternative for mapping rice area and forecasting its production, as it covers a large geographic area, is available the year around, can provide efficient analysis, timely information, and has the capability to delineate detailed spatial distribution of area under rice cultivation (Mosleh et al., 2015). The remote sensing platforms can view the surface of the earth repetitively and provide imagery that has been used for forecasting rice production employing various GIS and RS based methods in different parts of the world. Modern application of remote sensing to agriculture is based on the theory that "morphological characteristics of the plants are related to the optical properties, as provided by William Alen and Harlod Gausman. These scientists also published high resolution spectral signatures of healthy and nutrient-deficient diseased plants of both natural and cultivated species. (Gausman & Allen, 1973; Gausman & Hart, 1974; Gausman, 1973; Gausman et al., 1975; Gausman et al., 1971; Gausman et al., 1974; Gausman et al., 1969).

The leaves of green plants show very low reflectance and transmittance in visible regions (i.e. 400 to 700 nm) and high absorption in NIR region (NIR, 700 to 1300 nm) of the electromagnetic spectrum respectively. The reflectance or transmittance of light is based on photosynthetic and accessory plant pigments as well as scattering at mesophyll cell wall interface of the plant. It is therefore possible to measure the difference in reflected light at various wavelengths of the EM spectrum, distinguish vegetation from soil, green and senescent vegetation, and vegetation species. This difference in reflectance properties between the two regions of EM spectrum have led to the application of remote sensing approaches for monitoring and managing of natural vegetation (Ashraf et al., 2011; Campbell, 2002). The sensors fitted on satellites can measure the reflected red and near-infrared light waves. Scientists have evolved vegetation indices by mathematical formulas (algorithms), using the raw satellite data of reflected light. Vegetation indices (VIs) are mathematical combinations of mainly red, green and infrared spectral bands. These indices are designed to identify the functional relationships between crop characteristics and remote sensing observations (Wiegand & Richardson, 1990). VIs describe the relative density and health of vegetation or greenness for each pixel, in a satellite image. VIs are the combination of various wavebands related to the vegetation canopy parameters. VIs are aimed at enhancing the vegetation signal while minimizing the solar irradiance and soil background effects. Among them, Normalized Vegetative Difference Index (NDVI) is the most commonly used VI. The NDVI is defined as the ratio of (NIR – RED) / (NIR + RED) (Campbell, 2002; Holm et al., 1987; Roderick et al., 1996). NDVI is the most preferred vegetation index as its values saturate during the growing season of plants and provide better estimation of intercepted light by canopies. Other vegetation indices for mapping cropland are shown in Table 2.1.

Table 2.1. List of common vegetation indices, and their mathematical formulae, which have been used in mapping and yield/production forecasting (Mosleh et al., 2015).

Index	Abbreviation	Formula	Reference
Normalized Difference Vegetation Index	NDVI	$\frac{\rho_{NIR} - \rho_{R}}{\rho_{NIR} + \rho_{R}}$	(Rouse et al., 1973)
Ratio Vegetation Index	RVI	$\frac{\rho_{NIR}}{\rho_{R}}$	(Jordan, 1969)
Enhanced Vegetation Index	EVI	$2.5 \times \frac{\rho_{NIR} - \rho_{R}}{\rho_{NIR} + 6 \times \rho_{R} + 7.5 \times \rho_{B} + 1}$	(Huete et al., 2002)
Soil-Adjusted Vegetation Index	SAVI	$\frac{\rho_{NIR} - \rho_{R}}{\rho_{NIR} + \rho_{R} + L}(1 + L)$	(Huete, 1988)
Land Surface Water Index	LSWI*	$\frac{\rho_{NIR} - \rho_{SWIR1}}{\rho_{NIR} + \rho_{SWIR1}}$	(Xiao et al., 2005)
Normalized Difference Built-up Index	NDBI	$\frac{\rho_{SWIR1} - \rho_{NIR}}{\rho_{SWIR1} + \rho_{NIR}}$	(Zha et al., 2003)
Triangular Vegetation Index	TVI	$\sqrt{\frac{\rho_{NIR} - \rho_{R}}{\rho_{NIR} + \rho_{R}} + 0.5}$	(Deering et al., 1975)
Difference Vegetation Index	DVI	$\rho_{NIR} - \rho_{R}$	(Clevers,1986)
Infrared Percentage Vegetation Index	IPVI	$\frac{\rho_{NIR}}{\rho_{NIR} + \rho_{R}}$	(Crippen, 1990)
Perpendicular Vegetation Index	PVI	$\frac{\rho NIR - \mathrm{a} \times \rho R - \mathrm{b}}{\sqrt{1 + a^2}}$	(Richardson and Wiegand, 1977)
Rice Growth Vegetation Index	RGVI	$1 - \frac{\rho B - \rho R}{(\rho_{NIR} + \rho_{SWIR1} + \rho_{SWIR2})}$	(Nuarsa et al., 2011)

Note: ρ is the surface reflectance values for blue (B), red (R), near infrared (NIR), Shortwave infrared (SWIR1 and SWIR2 are centered at ~1.64 and 2.22 µm respectively); L = 0.5; a (gain) and b (offset) are derived from NIR *vs*. RED scatter plot. * In fact, Gao, 1996 developed the LSWI first, however the name was normalized difference water index (NDWI) using SWIR1 centered at 1.24 µm.

Kamthonkiat et al., (2007) determined that the spectral bands characterizing crops biophysical variables have a strong relationship with crop characteristics in specific narrow bands. They identified the following spectral bands in this regard: the longer wavelength portion of the red (650-700nm), secondary cluster in the shorter wavelength of green (500-550nm), a particular section of the NIR (900-940nm), and the moisture sensitive NIR (centred at 980- nm). However, a 12 Narrow band sensor in the 350 nm to 105 nm range of the spectrum is used for optimum estimation of agriculture crops biophysical information.

Mosleh et al., (2015) have given a review of literature on the application of RS to rice area mapping and production forecasting, using optical and microwave imagery. They have discussed synergy between remote sensing-based methods and other tools, and their application at the operational level. They found remote sensing-based method quite encouraging, despite some limitations. They indicated that optical remote sensing imagery had relatively low spatial resolution that caused inaccuracies in estimation of rice areas. Radar imagery on the other hand suffers from speckles and interacting surfaces that adversely affect the quality of images. They concluded that most of the methods used in forecasting rice yield were empirical in nature. Hence, they required further calibration and validation prior to their application in other geographical locations. They have discussed changes in NDVI during different growing stages of rice plants. They have also discussed importance of synergy between RS- Based methods and other parameters like metrological factors.

Prasad et al., (2007) have used a combination of vegetation indices and metrological parameters for forecasting crop yield in India. They derived an empirical equation to predict yield of wheat and rice. This equation and its coefficient look promising for predicting crop yield. Ahmad et al., (2014) estimated wheat crop yield using remote sensing technique and compared the results with crop reporting survey of Punjab. They argued that the remote sensing technique gave a reliable yield estimates. Siyal et al., (2015) used Landsat imagery time series for forecasting rice yield/production for Pakistan in Larkana district, Sindh, Pakistan. They observed high co-correlation between peak NDVI and observed rice yield for the years 2006-2013. However, RVI did not perform as well. They concluded that the use of remote sensing data holds promise for timely and efficient yield and production estimates for rice. Dempewolf et al., (2014) studied forecasting of the yield of wheat in the province of Punjab from vegetation indices and historic crop statistical data. The study used freely available MODIS and Landsat time series imageries approximately 6 weeks before the harvest. They derived wheat yield by regressing reported yield values against MODIS-derived vegetation indices of four different peak seasons. Among the four evaluated indices, WDRVI provided more persistent, accurate yield forecasts compared to NDVI, EVI2, and saturation adjusted SANDVI. Mccloy et al., (2007) evaluated two classification methods using four Landsat MSS images. The images comprised of G, R, and two NIR spectral bands that were acquired during the transplantation to canopy development stages. The first was acquired using Maximum likelihood classifier technique for generating the rice maps. The second image related to the use of vector classifier technique using two nodes (i.e., water and green canopy response). He found the vector classifier technique had produced better results. Yi-Siang Shiu et al., (2012) used two images consisting of four bands (R, G, B, and NIR) that were acquired during transplanting and tillering stages. For image classification, they used GIS Object-Based Post Classification (GOBPC) and pixel-based hybrid unsupervised and supervised classification. They found that GOBPC was more effective than the pixel-based classification. Fang., (2010) used one image of Landsat TM for rice crop in its early growing stage. He employed unsupervised classifier in two ways: (i) classification of the image after cutting out the study area (ii) classification of the entire image and then cutting out of the study area. He found that the second method was more accurate. Kamthonkiat et al., (2007) developed a “peak detector algorithm” to differentiate between rain-fed and irrigated rice crops. They used 10-day composite NDVI images over a period of three consecutive years and determined cropping intensity in Suphanburi, Thailand. They correlated the peak NDVI-values with the long-term average rainfall regimes. They found that the rain-fed rice had a “single” peak NDVI, while irrigated rice had “multiple” peaks. The overall accuracy of the outcome was 89%.

2.4 Model based Forecasting:

Crop Simulation Models (CSM) are computerized model that determine crop growth, development and yield, using mathematical equations to simulate functions of soil conditions, weather and management practices (Hoogenboom et al., 2004). CSM have played important role in the interpretation of agronomic results. Their application as decision support system for crop management is therefore on the increase.

CSM can be broadly classified into two groups: deterministic and stochastic. Deterministic models produce a specific outcome for a given set of conditions, assuming uniformity in plants and soils within the given area. Deterministic crop models can be classified into three basic types: statistical, mechanistic, and functional. Stochastic models produce outcomes when uncertainty associated with simulations has to be incorporated. Basso et al., (2013) have carried out review of crop yield forecasting methods, early warning systems and discussed the deterministic models in detail. An overview of the three models is given below.

2.4.1 Statistical models

Statistical models had been traditionally used for large-scale yield simulation. The crop yield trends were determined by regressing average yield from large areas against extended period. An upward trend in crop yield had been observed, though because of the use of better technologies and improved management practices. The biggest variable in these models was the weather data. The results of statistical models could not be extrapolated to another region and time because of the variation in soil, landscape, and weather conditions. They however provide useful insight about past yield and historical influences.

2.4.2 Mechanistic models

Mechanistic models give specific outcomes using fundamental mechanisms of plant and soil processes. They simulate photosynthetic processes, respiration including loss of CO_2 and production of biomass. They also simulate the dynamics of water in soil involving infiltration, evaporation, drainage, and root uptake. Because of more detailed inputs at the process level, the model becomes more complex and time consuming. However, better computing capability of new machines have improved their viability. Mechanistic models are not often used for problem solving purposes. They have greater academic utility and help in better understating of specific processes and interactions.

2.4.3 Functional models

Functional models have simplified the simulation of complex processes. Many functional models use biomass production per unit of radiation intercepted as a measure of the energy intercepted by the crop and it usually produces reasonable results when compared with the field measurements. These models when properly tested can provide appropriate details needed for assessing several issues affecting crop production. Functional models are now routinely used in Decision Support System (Basso et al., 2013; Hoogenboom, 2000; Motha, 2011).

CSM can improve understanding of the underlying processes, and highlight the areas of weakness. It thus supports strategic agricultural research. The knowledge-based systems approach can help in making good agricultural management decisions, taking into account the impact of anticipated climatic changes (Jame & Cutforth, 1996). CSM factor in weather data, soil fertility, and cultivar data and management practices and have therefore been used in the past to determine yield of major crops. This model is based on empirical evidence and hence is limited in its modelling application to a given area, because of the variation in weather data and soil fertility over large regions. However, despite its limitations, CSM are quite useful for comparative studies.

Advances in technology have now helped in the development of complex and simple CSM crop simulation models. CSM use information of several aspects regarding crop management, soil, and atmosphere. The level of complexity in the data ranges between hourly, daily and weekly inputs. Minimum DATA Set (MDS) is defined as the minimum amount of input data needed to run a CSM at a given site. MDS relates to site description, weather, soil, crop rotation, field managements covering details of cultivar, planting dates, irrigation practice and fertilizer application. (Basso et al., 2013; Hoogenboom, 2000)

A number of simulation models are available but the one that has been used by many is DSSAT-CSM, because it is more reliable and accurate in yield forecasting. DSSAT-CSM is an effective tool for field-level crop management and it helps users to integrate technical knowledge of these models with economic considerations and environmental impact assessment. It facilitate economic analysis and risk assessment of farming enterprises (Hoogenboom et al., 2004). Jones et al., 2003 have given details of crop simulation models namely DSSAT-CSM. An international network of scientists working on International Benchmark Sites Network for Agro Technology Transfer originally developed the DSSAT. The aim was to facilitate the application of the crop model using systems approach to agronomic research. DSSAT comprises a number of independent programs that operate around the CSM core. The input data relates to metrological conditions, experiment measurements, soil characteristics and the parameters of genotype information of the crop. The users employ software to prepare data input files and feed them to the system for generating simulated results. They compare the observed data to develop confidence in the system and determine modifications to improve accuracy. DSSAT-CSM helps in risk assessment and crop management by providing simulated options. The current model covers over one and half dozen crops that include wheat, maize, rice, potato etc.

DSSAT-CSM aims at three aspects of crop management. Firstly, simulation of monocrop production system is undertaken by incorporating data inputs regarding weather, genetics, soil water, soil carbon and Nitrogen etc, the outcomes also help in crop management covering one or more seasons, taking due cognizance of crop rotation at the given site. Secondly, it links modules of other abiotic and biotic factors with the programmer core. Thirdly, it helps in comparing alternative modules for making improvements, facilitating evolution, and preparing documentation. Lastly, it enables the introduction of CSM into other application programs. The DSSAT-CSM simulates crop growth and yield prediction on a uniform area of land under given weather and management practices by taking into account the variability of soil, water, carbon, and nitrogen over a certain period of time covering the cropping system.

2.5 An Integrated Approach of Yield Forecasting with GIS & RS and Crop Modeling

This approach combines the use of crop simulation models, national yield statistics, weather monitoring, RS and other information. The integration of RS and CSM for crop yield forecasting has been used for almost three decades. RS can quantify crop statistics at specific growth stages during the crop-growing season, while CSM can describe crop growth every day throughout the season. RS indirectly can provide measure for canopy state variables used by the CSM as well as both spatial and temporal information about those variables, which can then be used to adjust the model simulation. Algorithms are now available to estimate canopy state variables like LAI, vegetation fraction, and fraction of a PAR (Photosynthetically Active Radiation). One of the main integration procedures between the RS and CSM is the one that focuses on the adjacent LAI simulated with the crop model and the one estimated through RS. LAI (Leaf Area Index) is an important parameter because the leaves help in the exchange of water and CO_2 between the plant and the atmosphere. LAI is also used to model crop Evapotranspiration, biomass accumulation and final yield. Researchers working on such integration have generally adopted three basic steps: 1) estimate canopy variable with RS; 2) run the CSM: 3) use a proper integration method to adjust the model runs. The first step can affect the subsequent results of the integration because, if the crop variable are not properly estimated, adjusting the model with biased variables will lead to a wrong model evaluation.

An important step in the integration of crop model and RS is the use of the right technique to combine them. Scientist have mentioned four ways of integrating RS with CSM. A key point for successful integration of RS and CSM for in-season and between-season crop management is that the whole system, defining RS observation, crop simulation and soil-crop-weather, is properly understood. One of the most challenging problems in the combined use of CSM and RS is to interpret, understand and evaluate the results to develop the optimum agronomic management strategy that minimizes the variation in forecasting crop production.

Factors affecting crop growth, development and yield are well understood and evidence of yield variability is normally provided but not explained. The integration of RS and CSM is viable as CSM is good for understanding crop temporal variability, while RS maps the actual crop spatial variability at a given time during the growing season. Biomass production too links RS and CSM, as crop biomass is a function of the amount of Photosynthetically Active (solar) Radiation (PAR) absorbed in a given temperature and soil conditions. The amount of absorbed solar radiation is a function of the incoming radiation and capability of the crop to intercept and absorb it. That is mainly a function of the LAI (Baret & Guyot, 1991; Daughtry et al., 1992; Frouin & Pinker, 1995; Gallo et al., 1985; Garbulsky et al., 2011; Sellers et.,1992; Tucker & Sellers, 1986). fAPAR is quantified from RS because it can be predicted with the help of NDVI (Baret & Guyot, 1991).

Sufficient literature exists on yield forecasting and giving early warning of possible food shortage in a particular region. A crop failure and the consequent food shortage may be caused by drought conditions or climate change. Hence, timely yield forecasting is extremely important for ensuring food security in a particular country or region (Basso et al., 2013).

Chapter 3

MATERIALS AND METHODS

In order to forecast the yield of rice in Sheikhupura district, a combination of two approaches i.e. remote sensing and crop modeling was used and validated with field observed yield. The succeeding paras therefore give characteristics of the study area, its environment, details of the materials used and explanation of the methodologies applied in the two approaches.

3.1 Rice Production Zones and Cropping Pattern in Pakistan

In Pakistan, rice is grown in four distinct geographical and agro-ecological zones. Brief description of each zone is as follows:

The zone-1 covers flat valleys and terraces in the Northern mountainous areas of the country. The crops are mostly rainfed. The climate is sub-humid with average rainfall of 750 to 1000 mm in this area, mostly concentrated in summer. Low atmospheric temperature as well as cold water flowing down the streams sometimes causes damage to the rice crop. Water temperature in streams seldom exceeds 18 °C. The weather conditions cause leaf yellowing in early vegetative stage, delayed heading and sterility in the reproduction stage. The area is not suitable for high yielding rice varieties and Basmati rice. Wheat, berseem, barley, onion are grown in rotation with rice.

The zone-2 comprises the plains of Punjab lying between rivers Ravi and Chenab. A combination of canal water, sub soil water and a rainfall of 400-700 mm irrigate the crops. The area is suitable for growing fine aromatic Basmati as well some IRRI varieties. Rice is rotated with wheat, berseem and sunflower here.

The zone-3 primarily lies on the west bank of river Indus. It is canal irrigated but receives additional rainfall of about 100 mm. Despite high water table, the soil is suitable for rice crop. In this zone, rice is rotated with a variety of crops, especially gram, wheat/barley, oilseed, pulses and berseem/alfalfa.

The zone-4 comprises the Indus delta that has vast spill flats and basins, most of which are irrigated. The climate is arid tropical marine with almost no seasonal change. It is suitable for rice that is rotated with wheat, berseem and pulses (http://edu.par.com.pk/wiki/rice/).

3.2 Study Area

Sheikhupura district was selected as a study area for this research. It is major rice growing area of Punjab, Pakistan (Figure 3.1). It is situated at 31.71° North latitude, 73.98° East longitude with an elevation of 214 m above msl. It is part of Rachna Doab (the area lying between Rivers Ravi and Chenab). Sheikhupura district has deposits of calcareous alluvium derived from a wide variety of Himalayans rocks. The contributing rocks are calcareous sandstones, shales, clays, and igneous and metamorphic rocks such as granites and schists, genesis and slates. The soil texture generally comprises of loam and clay loam. Its organic matter content varies between 0.4 - 2.1%. The pH value of soli varies from 7.2 – 8.2 and its EC ranges between 1.1-9.9 mS cm $^{-1}$.

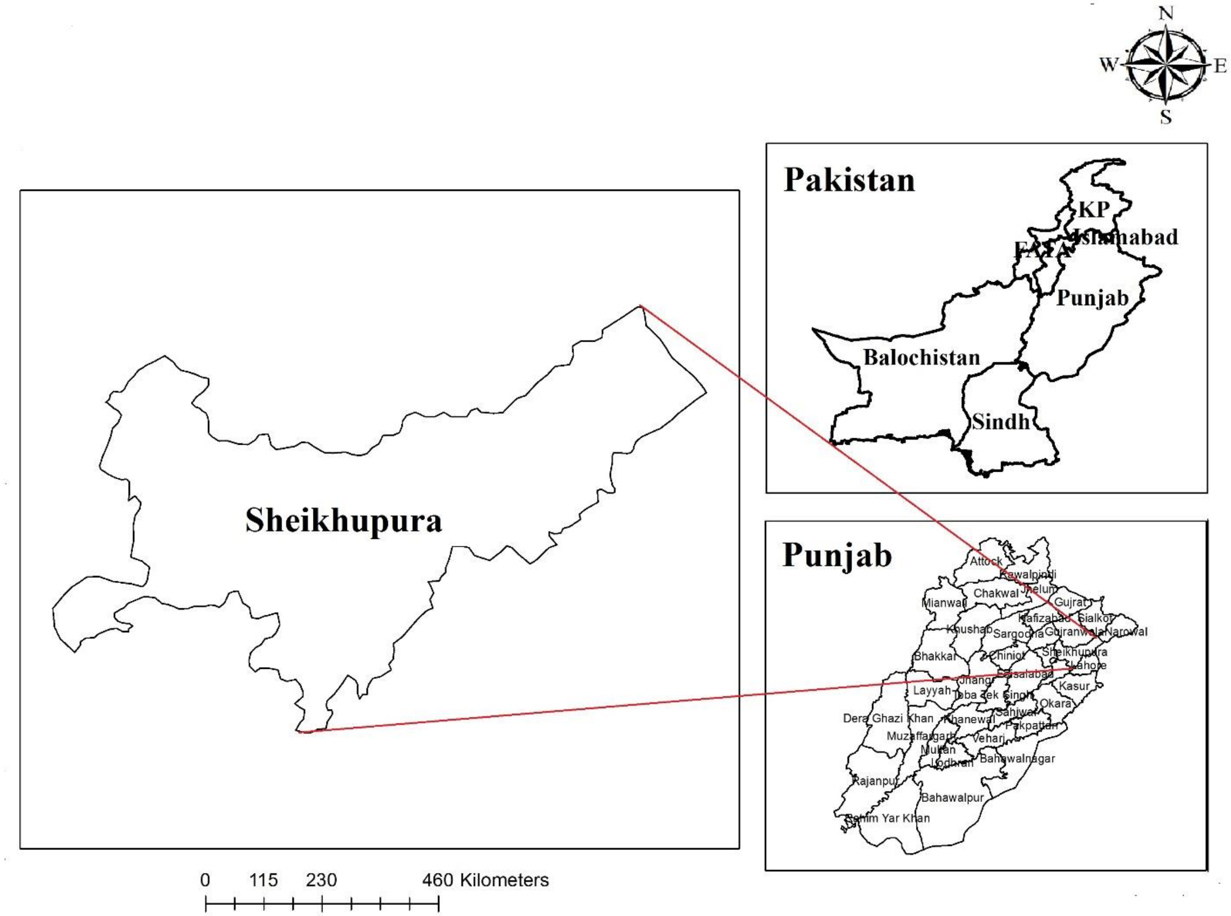

Figure 3.1. Map of study area showing map of Pakistan, map of Punjab and map of district Sheikhupura.

The availability of phosphorus and potassium ranges between 3.1 to 8.3 mgkg^{-1} and 43 to 350 mg kg^{-1}, respectively (Soil Survey of Pakistan, 1960).

The district has extreme climate; the summer season starts from April and continues till October. During the summer season, temperature ranges from 30 to 45 °C. The winter season starts from November and continues till March. December and January are the coldest months with a mean minimum temperature of 5 °C. The dust storms occur occasionally during the hot summer months of June, July and August. Rainy weather alternates with oppressive weather. The total rainfall is 500 mm per year. The mean minimum and maximum humidity during winter is 37% and 84%. Irrigation water quality, quantity and method of its application impact production of rice significantly. An irrigated rice crop cycle requires from 1200-1800 mm water during the growing season. The main supply of water is through irrigation canals and tube-wells. Sheikhupura district is irrigated by Upper Chenab Canal (UCC), Gugera Branch and Lower Chenab Canal (LCC) (Source: http://pakcities.com).

The major crops grown in Sheikhupura are wheat, rice and sugarcane. Rice is an annual grass with round, hollow, jointed culms; narrow, flat, sessile leaf blades joined to the leaf sheaths with collars. There are three stages of growth of rice, namely vegetative stage, reproductive stage and ripening stage (Figure 3.2). It starts with germination and ends at panicle initiation. It includes seedling, transplantation, and tillering and photoperiod sensitive stages of rice. It usually take 55 to 85 days to complete. The reproductive stage includes the period during which panicles form and enlarge from the base of the tillers. It lasts for 45 days among all varieties of rice. It is further divided into booting stage, heading stage and flowering stage. The booting stage is high in its demand for nutrients as it involves rapid growth of plant. It takes 15 to 20 days. The heading stage takes about 10 days and about 90 % panicles emerge

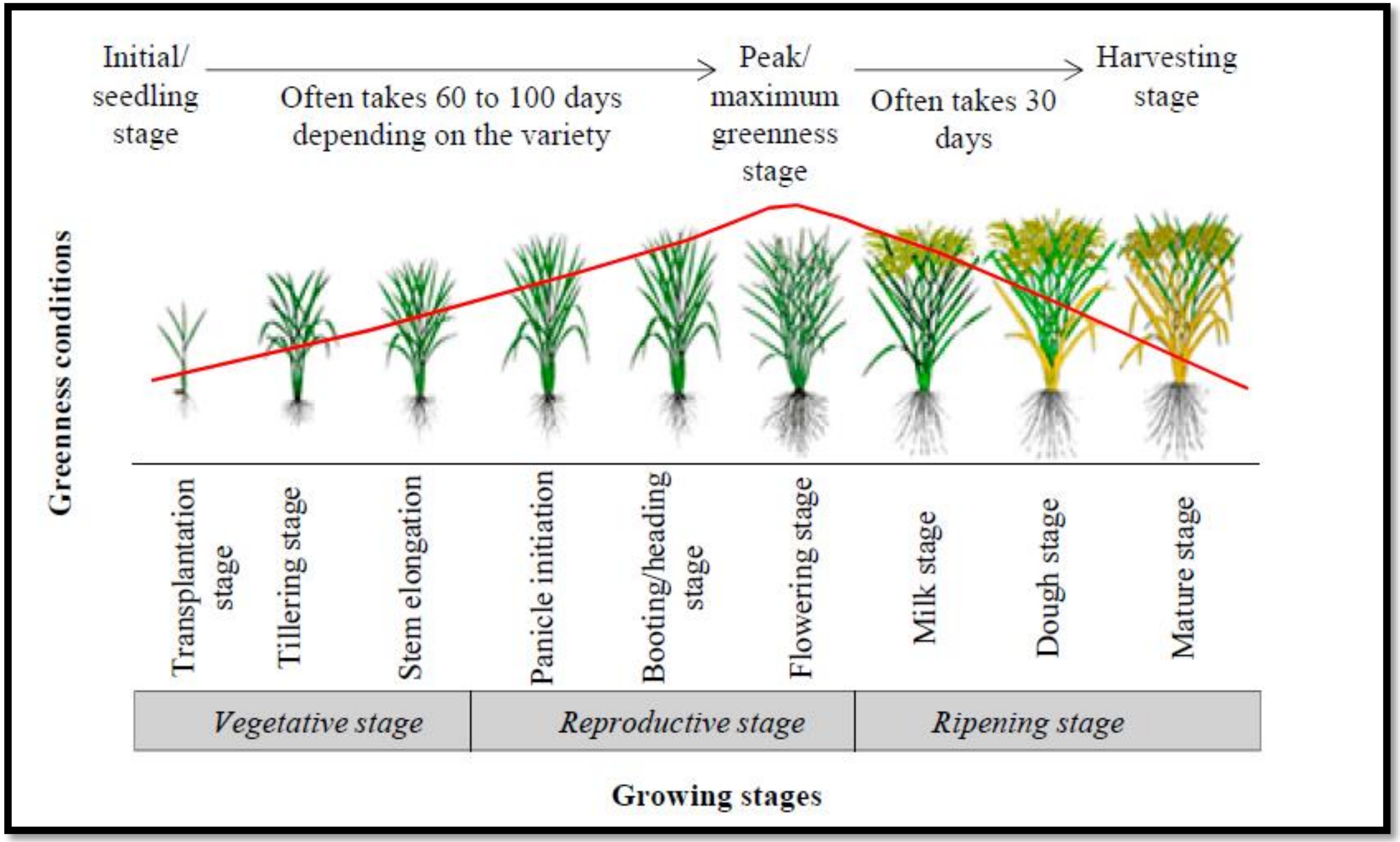

Figure 3.2. Growth stages of a typical rice crop and their associated greenness conditions (Mosleh., 2015).

during heading. The ripening stage comprises grain-filling and ripening phase over a period of about 25 to 35 days. Ripening can further be broken into the milk stage, the dough stage, the maturity stage and over ripe stage. Rice is vulnerable to pest attack during the milk stage. Birds join pests in dough stage and have to be warded off. At maturity, the grains ripen but the leaves start turning yellow, allowing nitrogen to feed the grains rather than the leaves. Full maturity implies that more than 90% grains have become ripe. The farmers must harvest the crop before it over ripe, as in the over ripe stage vegetative part starts to die off and grains start falling to the ground. Every additional day of over ripe stage is a loss to the production of rice (Source: http://ricepedia.org/rice-as-a-plant/growth-phases).

3.3 Methods of Rice Cultivation in Sheikhupura

There are two methods of rice cultivation i.e. broadcast sowing and transplantation. The broadcasting involves plantation by direct broadcasting of rice seeds in the field. While in transplantation, sowing of rice begins in nursery beds. The plants grow to a height of 4 to 6 inches, before they can be transplanted into the main field in rows with the plant-to-plant spacing of about 3 inches and inter-row distance of about 6 inches. It is the most scientific method that helps in increasing the crop production considerably. It is also referred to as the Japanese Method.

3.4 The Research Design

The research design aims at using research evidence to answer the research questions in as clear a manner as possible. The design of this research focuses primarily on the comparative accuracy, validity and effectiveness of rice yield forecasting using state of the art technologies and field surveys, capitalizing on the knowledge and evidence inputs. The research design calls for accuracy in results that in turn requires extensive data collection through reliable means and methods. It follows a combination of qualitative and quantitative methods of research. The Crop Simulation Model (CSM) needs inputs some of which are possible only through field surveys; otherwise, the model does not run. Likewise, the GIS & RS–based approach requires ground coordinates to peg RS data to the selected field points. While field surveys are based on qualitative research method, the CSM modules uses extensive data and is, therefore, based on quantitative approach (Figure 3.3).

3.5 Remote Sensing-Based Yield Forecasting

3.5.1 Field survey

Data on rice yields of growing season (July-November) was collected in 2015 by means of interviews with farmers regarding their production and a number of other parameters. A total of 33 sites were selected randomly for collecting field data (Figure 4.1). This data was used to develop a regression model of yield with spectral information from imagery (NDVI). The field survey was also essential for providing data input to the CSM. The collected field survey data included: Latitude and Longitude data of the selected field through global positioning system (GPS), particulars of the land owners/farmers including their total land holding (to determine their capacity to provide agricultural inputs for better yield/production), rice crop variety and amount of seed used per ha, method of irrigation, data on fertilizer application, information on crop rotation indicating the crop preceding rice, date of sowing and harvesting of rice, and actual estimated yield of the selected farm (Appendix 1).

3.5.2 Remote Sensing Data

The temporal data of Landsat 8 satellite imageries was downloaded covering time period from August to November 2015 (28 Aug., 13 Sep., 29 Sep., 15 Oct., 31 Oct., and 16 Nov.) Six imageries were downloaded corresponding to the different stages of growth and

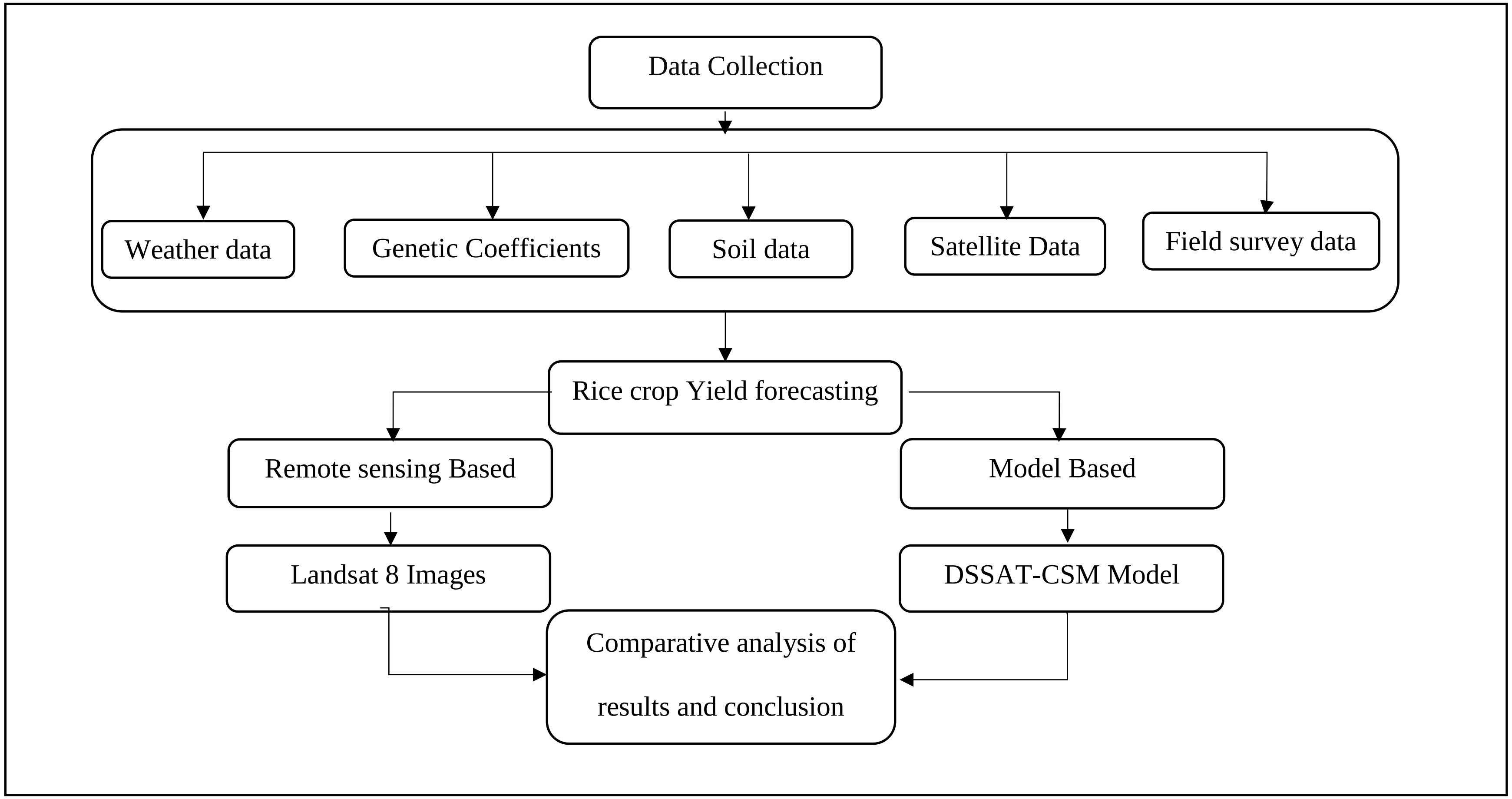

Figure 3.3. Schematic diagram of the proposed methodology.

development of the rice crop. Due to heavy monsoon rainfall and cloud cover in the month of July, the imagery covering the early growth period did not offer much of information and was therefore excluded from the study (Table 3.1).

3.5.3 Methodology

The Temporal Landsat 8 imagery from July to November 2015 was used for preprocessing using ENVI and ERDAS IMAGINE (Table 3.1 & 3.2). During preprocessing, six bands of the spectrum ranging from 0.45-2.29 μm were stacked. FLAASH model of ENVI software was used for atmospheric correction. It provided accurate derivation of apparent surface reflectance. FLAASH operates in 0.4–2.5 μm spectral range, and corrects wavelengths in the visible through NIR and shortwave infrared regions. It incorporates the MODTRAN4 radiation transfer code, and provides correction for the adjacency effects, computation of scene average visibility, cirrus and opaque cloud classification maps and adjustable spectral polishing for artifacts separation. Water vapors and aerosol retrieval are only possible when the image contains bands in appropriate wavelength positions. The software can correct images collected in either vertical or slant-viewing geometries. (Agrawal et al., 2005; Cooley et al., 2002; Matthew et al., 2002).

The study area was extracted using boundary shapefile of Sheikhupura district. The NDVI of all the images was calculated by using the formula given in Equation 1. NDVI is widely used vegetation index related to canopy biomass for all growth stages of the plants (Aparicio, et al., 2000; Reyniers, et al., 2004; Royo, et al., 2003). NDVI has been related to nitrogen status, chlorophyll content, green leaf biomass, and grain yield of the crops (Shanahan, et al., 2001; Solari, et al, 2008).

Table 3.1. List of Landsat 8 scenes. Acquisition dates covering from early growth till crop harvesting.

Sr. No	Date of Acquisition	Path/row
1	28-Aug-2015	149/38
2	13-Sep-2015	149/38
3	29-sep-2015	149/38
4	15-Oct-2015	149/38
5	31-Oct-2015	149/38
6	16-Nov-2015	149/38

Table 3.2. List of softwares used in study.

Sr. No	List of Software Used
1	Arc GIS 10.2
2	ERDAS IMAGINE
3	ENVI

It is a combination of addition, subtraction and division of absorption (red) and reflectance (infrared) bands (Holm et al., 1987; Roderick et al., 1996).

$$NDVI = (NIR - Red) / (NIR + Red) \ldots\ldots\ldots\ldots\ldots\ldots\text{ Equation 3.1}$$

To discriminate the rice crop from other vegetation ArcGIS CON-Tool was applied on NDVI raster using the minimum-maximum NDVI values of rice crop identified during the field survey. This resulted a masked NDVI raster of only rice crop fields. The masked NDVI raster was then used to develop a regression model between NDVI and rice crop yield of selected field sites.

In order to establish a more accurate relationship between the yield of the selected fields and their NDVI, the area around each selected point was expanded to cover nine pixels in the 3 x 3 pixels polygon, surrounding the selected point (Figure 3.4a). A mean of NDVI values of all nine pixels was calculated and regressed to determine its relationship with the reported yield (About 4.5 pixels cover an area of one acre on ground. Since the farmers had reported their yield per acre, each figure was divided by 4.5 to get average yield of each pixel). In order to achieve greater accuracy in determining the correlation between NDVI and yield, the entire process was repeated by selecting four highly correlated pixels out of nine selected in the first stage (Figure 3.4b). The mean of the most correlated NDVI values of the set of four pixels were plotted against the yield of 33 sites of all the images to determine the most correlated NDVI-Yield Values. The entire process led to the determination of peak season of the rice crop. By applying CON-Tool in Arc GIS 10.3.1, the minimum-maximum values of NDVI for rice crop were used in the identification of pixels covering the rice crop area. A new raster showing the NDVI of rice crop only was then generated and used with the regression equation

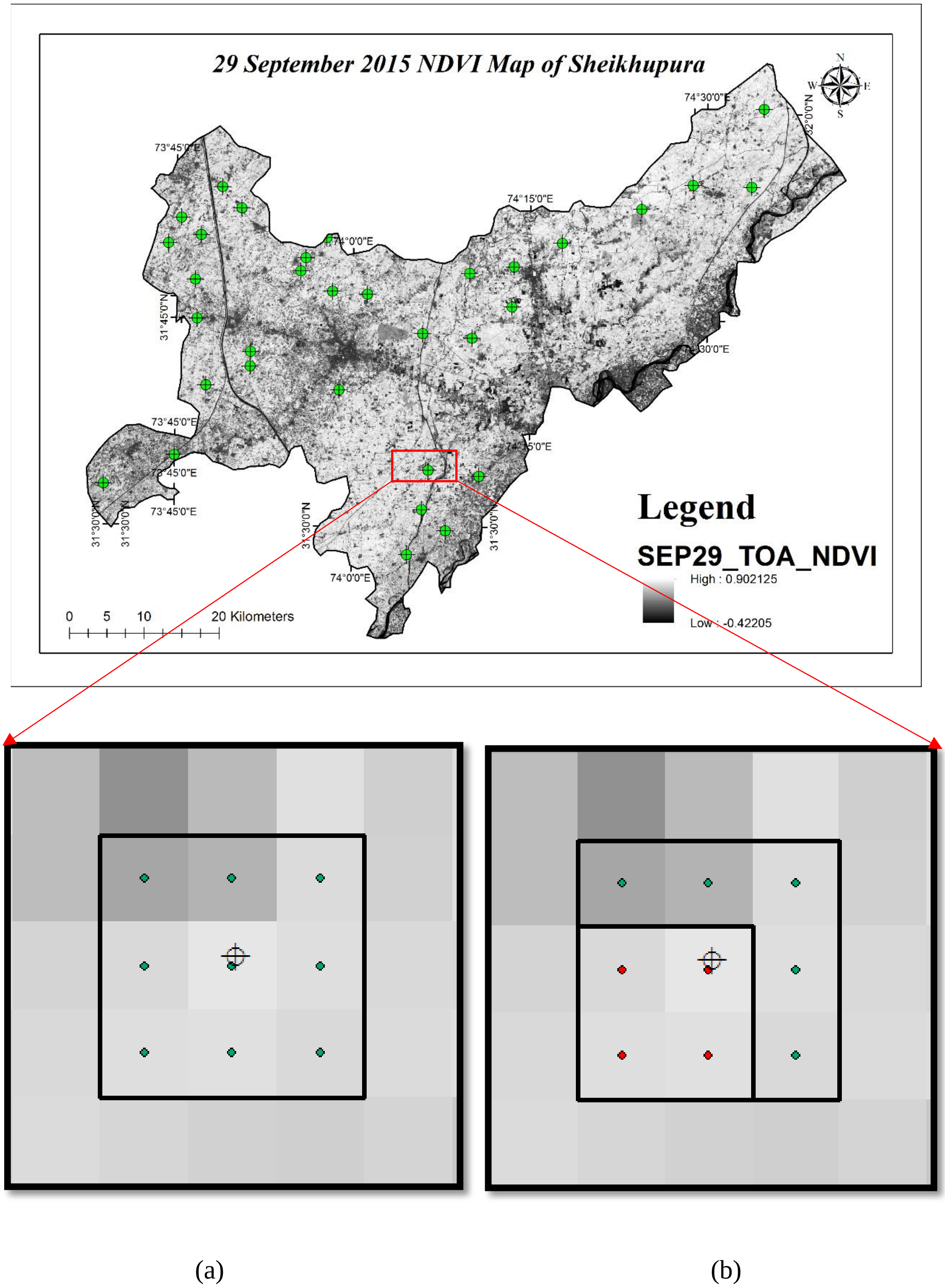

Figure 3.4. Highly correlated pixel selection for regression analysis. (a) Highly correlated nine pixel (b) Highly correlated four pixels out of nine.

created earlier to compute the yield of each NDVI pixel of rice using the raster calculator. A new raster showing rice crop yield of district Sheikhupura was generated. The flow chart given in Figure 3.5 gives the methodology at a glance.

3.6 CERES-DSSAT Model Based Yield Forecasting

3.6.1 Model description

The DSSAT comprises a number of independent programs that are integrated to operate together and simulate growth and development of crop over the given time. It also takes into account the soil water, carbon and nitrogen process and management practices. Figure 3.6 shows the main components of DSSAT-CSM. These include:

- A main driver program, which controls timing for each simulation.
- A Land unit module that simulates processes affecting the land units.
- A number of primary modules that simulate processes of individual units related to water, plant growth, soil processes, soil-plants atmosphere interface and management practices.

The component units collectively simulate the changes over time in the soil and plants occurring in a given land unit under the given weather conditions and management practices. The model helps the users in preparing databases related to weather, soil characteristics, genotype information and management for application under varying conditions. The results simulated by the model are compared with the observed data and calibrated. The DSSAT model is a good planning and management tool for working out the future management options, while taking due cognizance of the associated risks (Jones et al., 2003).

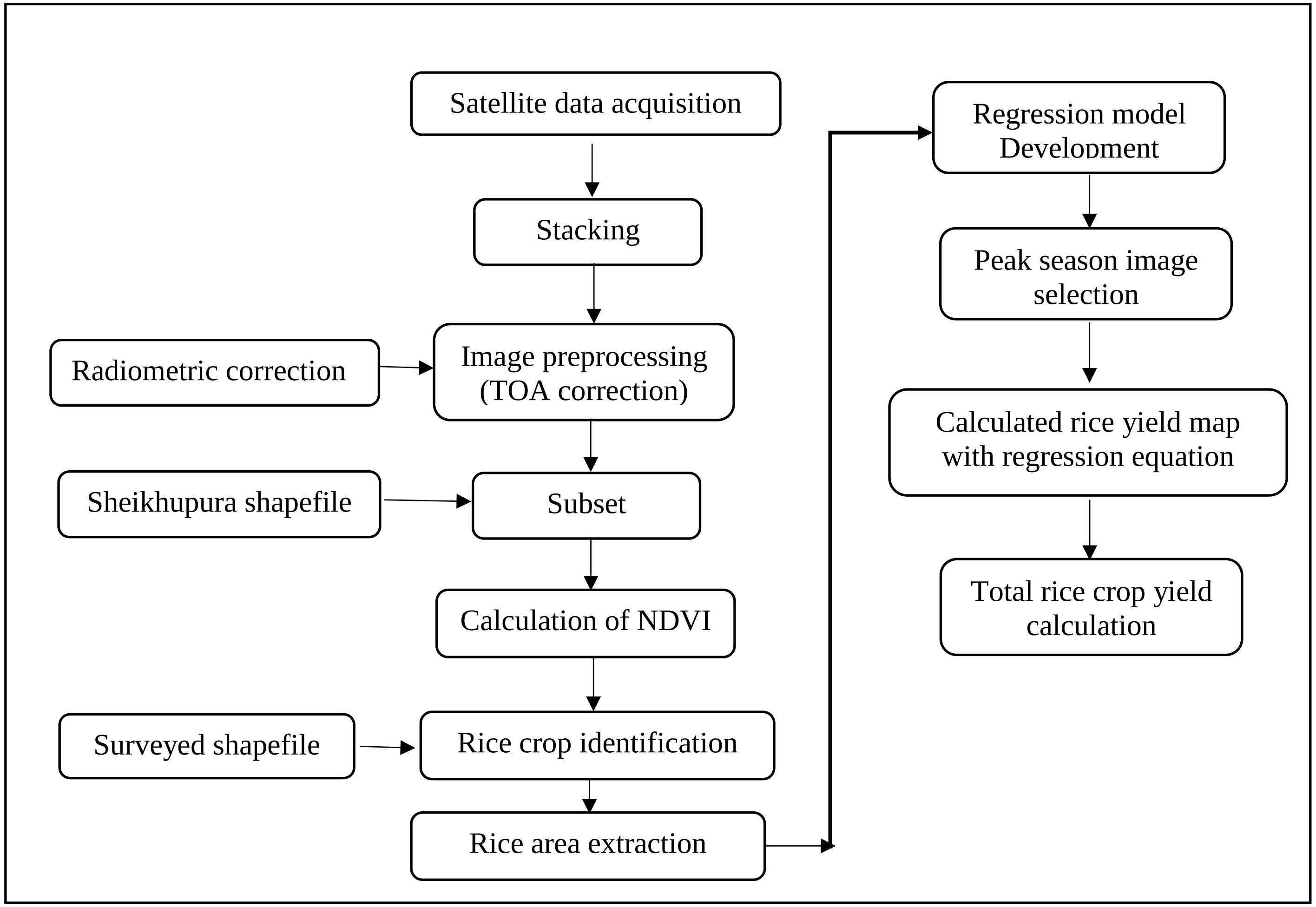

Figure 3.5. Schematic diagram of the proposed methodology of remote sensing.

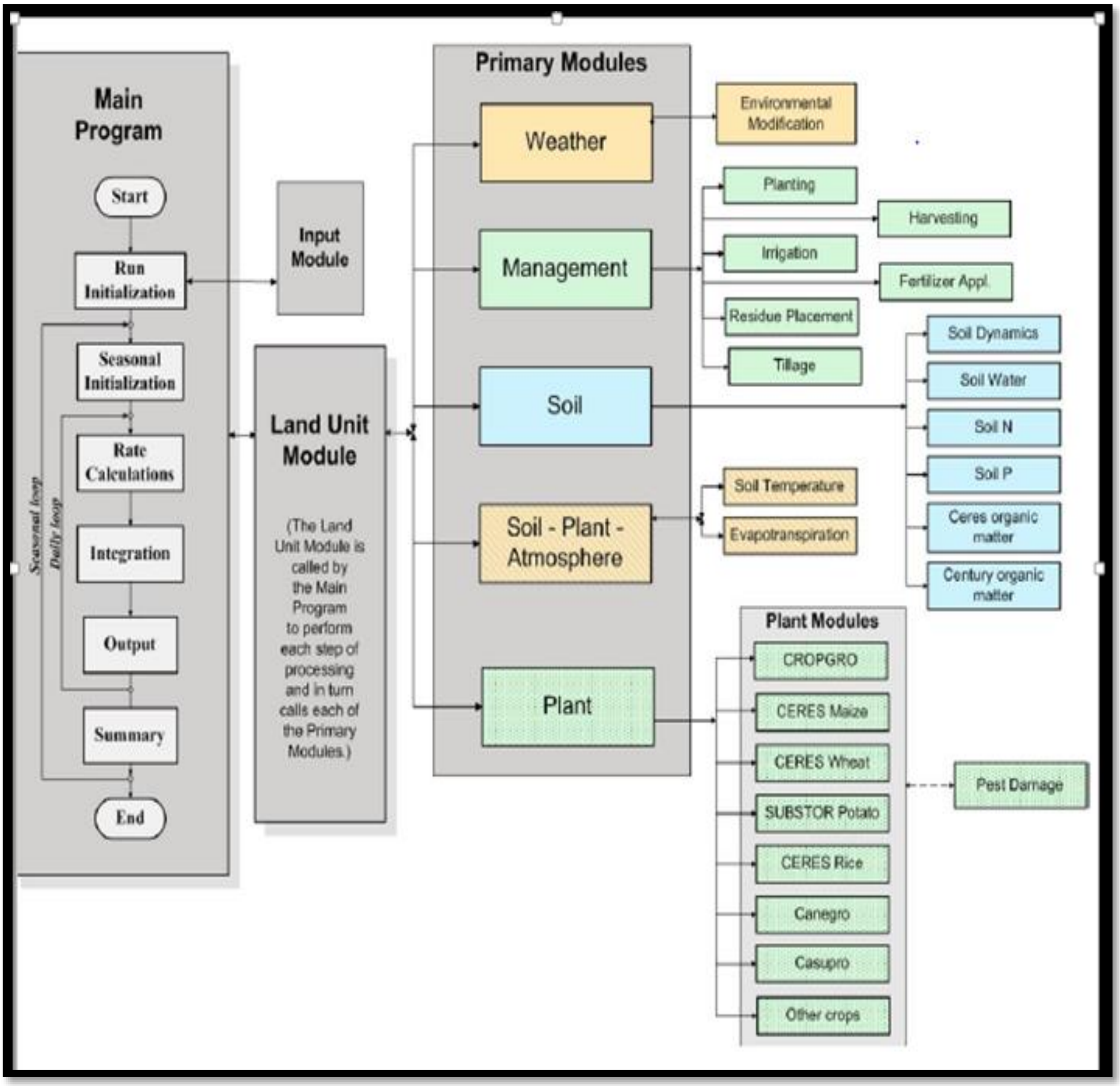

Figure 3.6. Overview of components and modular structure of DSSAT-CSM.

3.6.2 Input Data for DSSAT-CSM

Following inputs were provided to the CSM:-

- Metrological data
- Soil data
- Cultivar research data
- Management practices

3.6.2.1 Metrological data

The Sheikhupura district is covered by Lahore weather station/observatory of Pakistan Metrological Department (PMD). Metrological data of last thirty years (1985-2015) was obtained from PMD to have a large statistical base and hence more reliable metrological data inputs to CSM. The data covered daily Maximum & Minimum temperatures, rainfall and solar radiation. An initial analysis of the met data revealed that it was almost uniform across the spatial dimensions of the area of study.

3.6.2.2 Soil Data

The basic information on the land forms and soil series of the study area was obtained from the Soil Survey of Pakistan/Punjab. Some specific properties of soil fertility of the study area required by CSM are given in Table 3.3.

3.6.2.3 Cultivar data

The data of specific cultivar that is commonly sown in Sheikhupura was collected from Rice Research Center Kala Shah Kaku (KSK), Sheikhupura Punjab. This data was used to calibrate and validate the CSM for forecasting the yield of rice crop. The relevant cultivar data is given in Table 3.4.

3.6.2.4 Management Practices Input Data

Crop management includes the execution of field operations for the entire crop management cycle including crop rotation, sowing and harvesting dates, planting patterns giving rows-column spacing and application of fertilizer etc. This data was collected by field survey (Appendix 1).

3.6.3 Model Calibration and Validation

CERES-Rice model was manually calibrated using field data collected from Kala Sha Kaku Rice Research Institute (KSKRRI) during 2015 rice growing period. The genotypic coefficients were calibrated to match the model outputs with the field observed data. The details of genotypic coefficients have been presented in Table 3.5.

Validation of model was performed using independent data sets obtained from 33 different sites of Sheikhupura district. Validation skill scores such as R^2 and RMSE were used to check the performance of the model.

3.6.4 Validation of Remotely Sensed and Simulated Crop Yield

The validation skill scores like, Root Mean Square Error (RMSE) and coefficient of determination (R^2) were used to evaluate the performance of DSSAT-CSM model and remote sensing based Yield forecasting as given below:

Root Mean Square Error

$$RMSE = \sqrt{\frac{1}{n}\sum_{i=1}^{n}(Y_i' - Y_i)} \quad \text{..........................Equation 3.2}$$

Coefficient of determination (R^2):

$$R^2 = \frac{\sum_{i=1}^{n}(Y_i' - \bar{Y})^2}{\sum_{i=1}^{n}(Y_i - \bar{Y})^2} \quad \text{........................Equation 3.3}$$

Together with the above, where n is the number of comparisons; Yi is the Observed rice yield; $\bar{Y}$ is the average rice yield, and Y_i' is the predicted yield.

Table 3.3. Physical and chemical characteristics of soil at the experimental site.

	Depth (cm)				
Soil characteristics	**0-12**	**12-28**	**28-53**	**53-94**	**94-160**
Clay %	45	54	51	42	40
Silt %	38	35	31	39	41
Organic Carbon	0.56	0.5	0.47	0.21	0.1
pH	7.3	7.5	7.8	8	8.5
Bulk density (Mg-3)	1.31	1.32	1.32	1.33	1.34
CEC (cmol/kg)	22	19	15	21	18
Lower limit (mm)	0.266	0.31	0.294	0.242	0.229
Upper drained limit (mm)	0.414	0.456	0.429	0.482	0.373
Saturation (mm)	0.476	0.473	0.473	0.472	0.469
Satu. Hydraulic conduct, cm/h	0.06	0.06	0.06	0.06	0.09
Root Growth Factor 0.0 to 1.0	1	1	0.445	0.23	0.079
Total N (%)	0.08	0.06	0.03	0.01	0

Table 3.4 . Experimental data of the rice crop cultivar (PS2)

	Replications		
Character	**R1**	**R2**	**R3**
Plant Height (cm)	116	115	116
Tillers	14	14	14
Emergence Date	02-Aug-07	02-Aug-07	02-Aug-07
Days after Flowering	86	86	89
Days to Physiological Maturity	116	117	119
Days to Harvesting	125	125	125
Leaf Area Index(cm2)	48.34	45.43	46.65
Stem Length (cm)	100.1	97.3	99.7
Grains Per Panicle	83	100	96
1000 Grain Weight (g)	27.5	29	29.2
Panicle Length (cm)	27.5	26.4	27.3
Plot Area (m2)	15	15	15
Rows Per Plot	15	15	15
Plot Length (m2)	5	5	5
Plot Spacing (m)	0.2	0.2	0.2
Plot Layout	RCBD	RCBD	RCBD
Harvested Area (m2)	15	15	15
Harvested Row Number	15	15	15
Harvested Row length (m)	5	5	5
Harvesting Method	Manual	Manual	Manual
Yield (kg ha-1)	3430	3147	3237

Table 3.5. Genetic coefficients of the rice cultivar (PS2).

Genetic	Description	Coefficient Parameters
P1	Time period (expressed as growing degree days (GDD) in ◦C above a base temperature of 9 ◦C from seedling emergence during which the rice plant is not responsive to changes in photoperiod.	200
P20	Critical photoperiod or the longest day length (in h) at which the development occurs at a maximum rate.	156
P2R	Extent to which phasic development leading to panicle initiation is delayed (expressed as GDD in ◦C) for each hour increase in photoperiod above P20.	450
P5	Time period in GDD ◦C) from beginning of grain filling (3 to 4 days after flowering) to physiological maturity with a base temperature of 9 ◦C.	11.0
G1	Potential spikelet number coefficient as estimated from the number of spikelets per g of main culm dry weight (less lead blades and sheaths plus spikes) at anthesis.	40.0
G2	Single grain weight (g) under ideal growing conditions, i.e., non-limiting light, water, and nutrients and absence of pests and diseases.	0.027
G3	Tillering coefficient (scaler value) relative to IR64 cultivar under ideal conditions.	1.00
G4	Temperature tolerance coefficient. Usually 1.0 for varieties grown in normal environments.	0.80

Chapter 4

RESULTS AND DISCUSSION

4.1 Remote Sensing Based Yield Forecasting

4.1.1 Field Survey

Data on rice crop management was collected in 2015 by means of interviews of 33 farmers (Figure 4.1). A surface area of one acre was taken as the sample unit. These samples were used to develop a regression model of yield vs NDVI. The collected field survey data included the following: - Latitude and Longitude of the selected field through GPS to ground-check the Landsat 8 data (Figure 4.1 showing map of surveyed sites), particulars of the land owners/farmers including their total land holding (to determine their capacity to provide agricultural inputs for better yield/production), seed variety and amount of seed used per ha, method of irrigation, data on fertilizer application, information on crop rotation indicating the crop preceding rice, date of sowing and harvesting of rice to provide input to the DSSAT-CSM, and actual estimated yield of the selected farm for comparison with the calculated yield by RS and simulated yield by DSSAT-CSM (Appendix 1). Figure 4.2 shows photographs of farmers' interview in progress and field visits.

4.1.2 Derivation of relationship between temporal Imagery and growth stages of rice crop

Landsat 8 imageries covering the growth of rice crop from its early vegetation growth till its harvesting stage were analyzed (Figure 4.3). The sowing of rice started in July in this part of Pakistan. However, the imagery of July had extensive cloud cover and was therefore discarded. The next best image was that of 28th of August which too corresponded to the early growth stage of rice. It was therefore selected for analysis. The subsequent imageries of September, October and November were quite clear and were hence used for analysis. NDVI

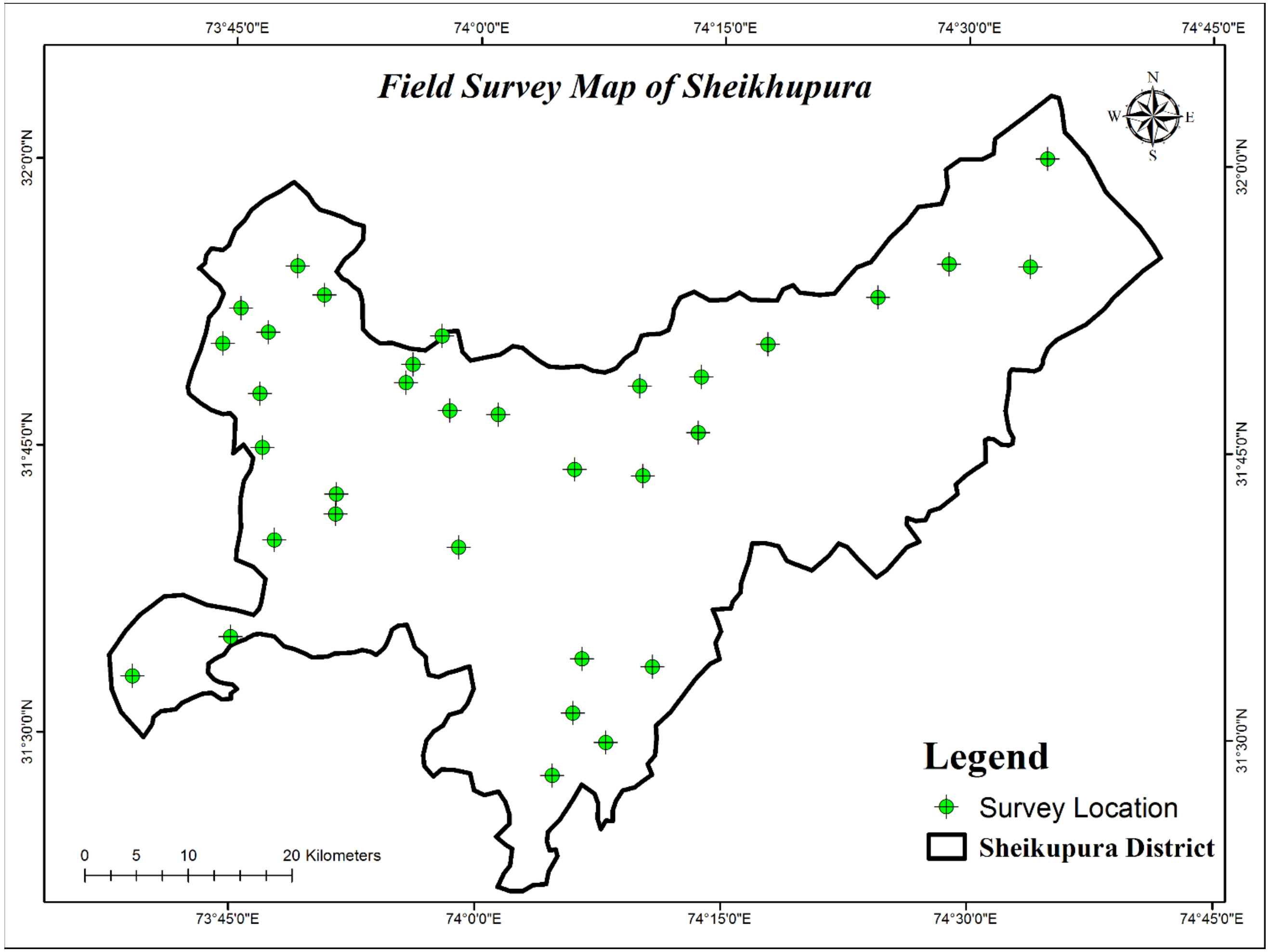

Figure 4.1. Field survey map of Sheikhupura.

Figure 4.2. Photographs showing farmers' interview and field visits in Sheikhupura district.

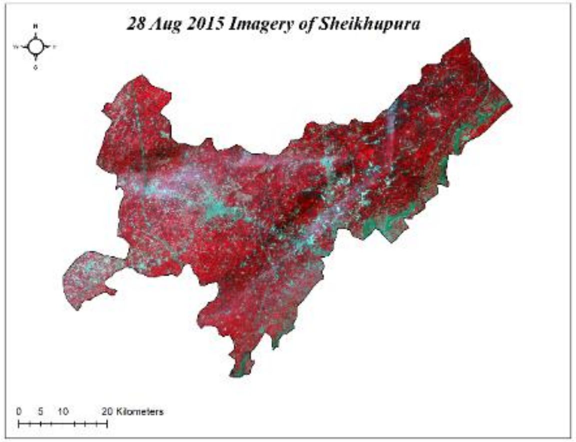

(a)

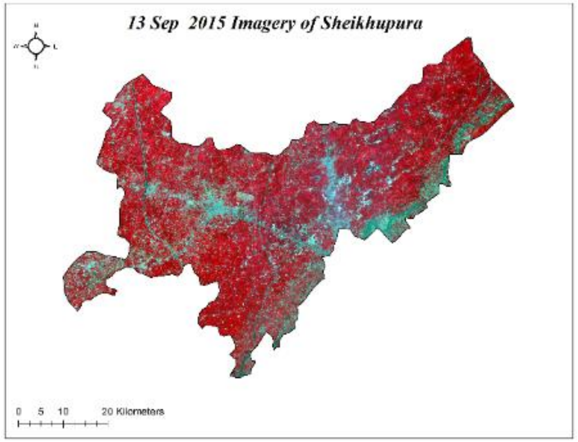

(b)

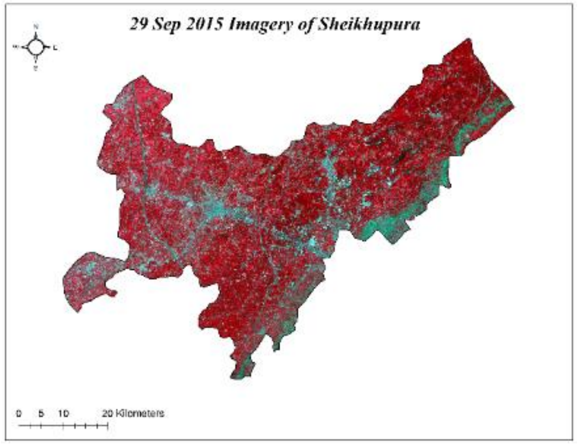

(c)

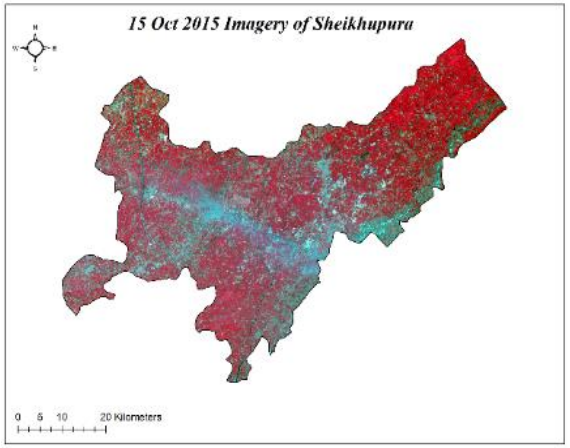

(d)

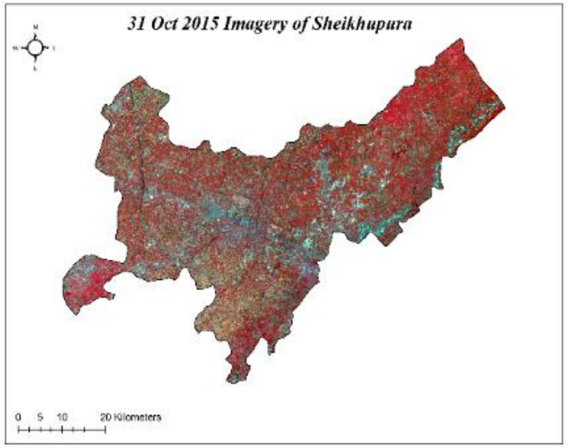

(e)

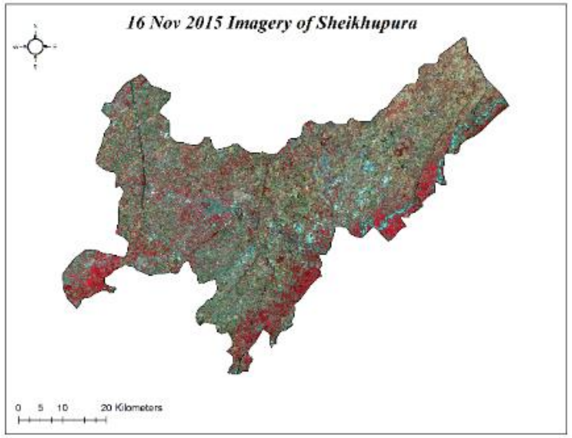

(f)

Figure 4.3. Landsat 8 imagery of phonological growth stages of rice: a) stem elongation stage b) booting or heading stage c) flowering stage d) milk stage e) dough stage f) ripening stage.

values of cultivated area observed on 28th August and 13th September were low. That could be attributed to the continuity of early vegetation growth stages. The factors that contributed to lower NDVI values of those images were lesser crop leaf area and influential background reflectance of soil in the red band (Serrano, et al., 2000). The highest NDVI values were observed on the imagery of 29th September that covered the maturity stage (Figure 4.4 & 4.5). In October the NDVI values started decreasing due to leaf senescence which caused increased reflectance in the red band. It may be added here that the spectral response of two different crops sown in a given area tends to be the same in visible and NIR range of electromagnetic spectrum, provided they are planted on the same date and they acquire maximum canopy cover simultaneously. This conflict was resolved by field survey/ground-check in which exact dates of sowing of rice crop, and field management practices were obtained.

4.1.3 Linear regression Model Development

The linear regression model was developed between the observed yield and mean NDVI Values of nine and four pixel sets of selected field sites. After observing the linear relationship between field yields and the six Imageries Mean NDVI values, the 29th September imagery showed the highest fit between NDVI and yield (Figure. 4.4 & Figure 4.5). However, the results of Four Pixels (FP) Mean NDVI values (Figure 4.5) were better correlated than Nine Pixels (NP) mean NDVI values (Figure 4.4). Hence, the regression model developed with FP mean NDVI values was used to calculate the Rice crop yield. The correlation between the rice grain yield and corresponding NDVI values during the early vegetative growth period in August was very low (R^2=0.0439) because of the reflectance from mixed pixels of rice, other vegetation and soil background. Subsequently the relationship between NDVI and rice grain

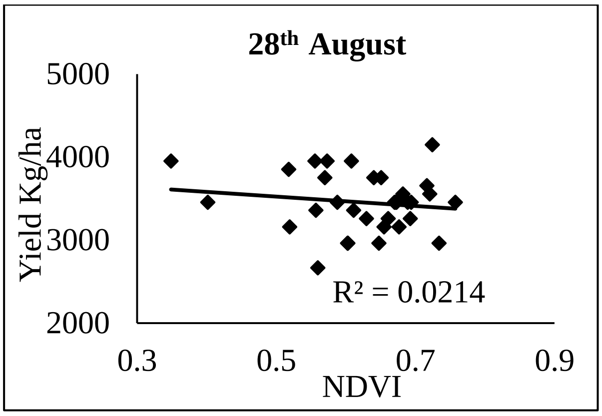

(a)

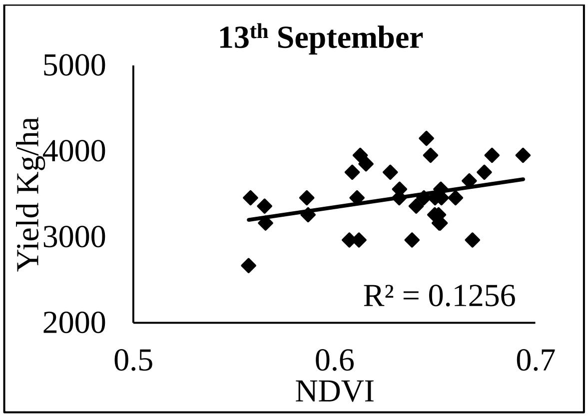

(b)

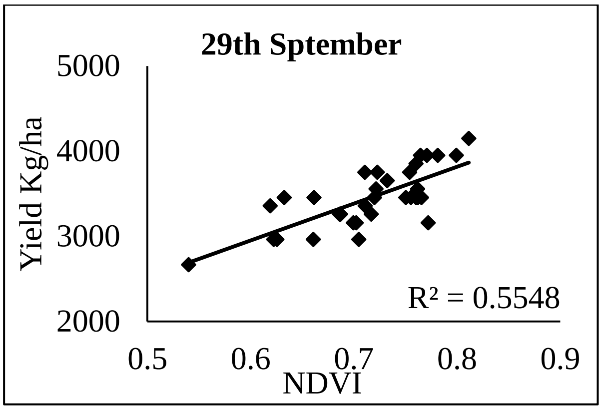

(c)

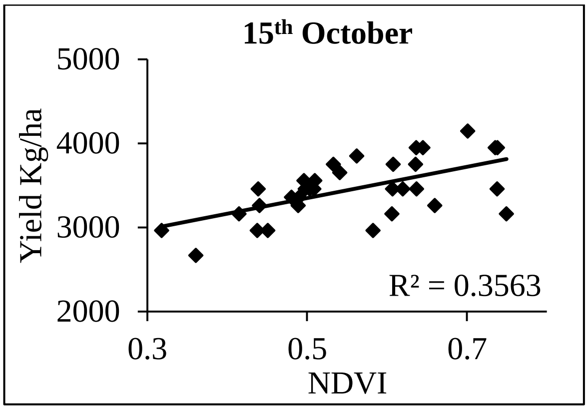

(d)

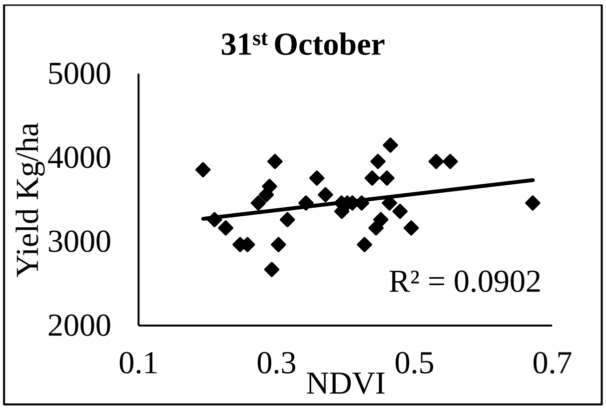

(e)

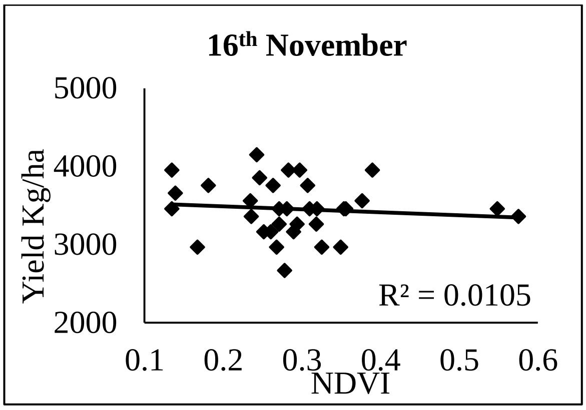

(f)

Figure 4.4. Linear regression curve showing relationship between Nine Pixels (NP) Mean NDVI values and Observed rice yield of 33 sites on: (a) 28^{th}August (b) 13^{th} September (c) 29^{th} September (d) 15^{th}October (e) 31^{st} October (f) 16^{th} November.

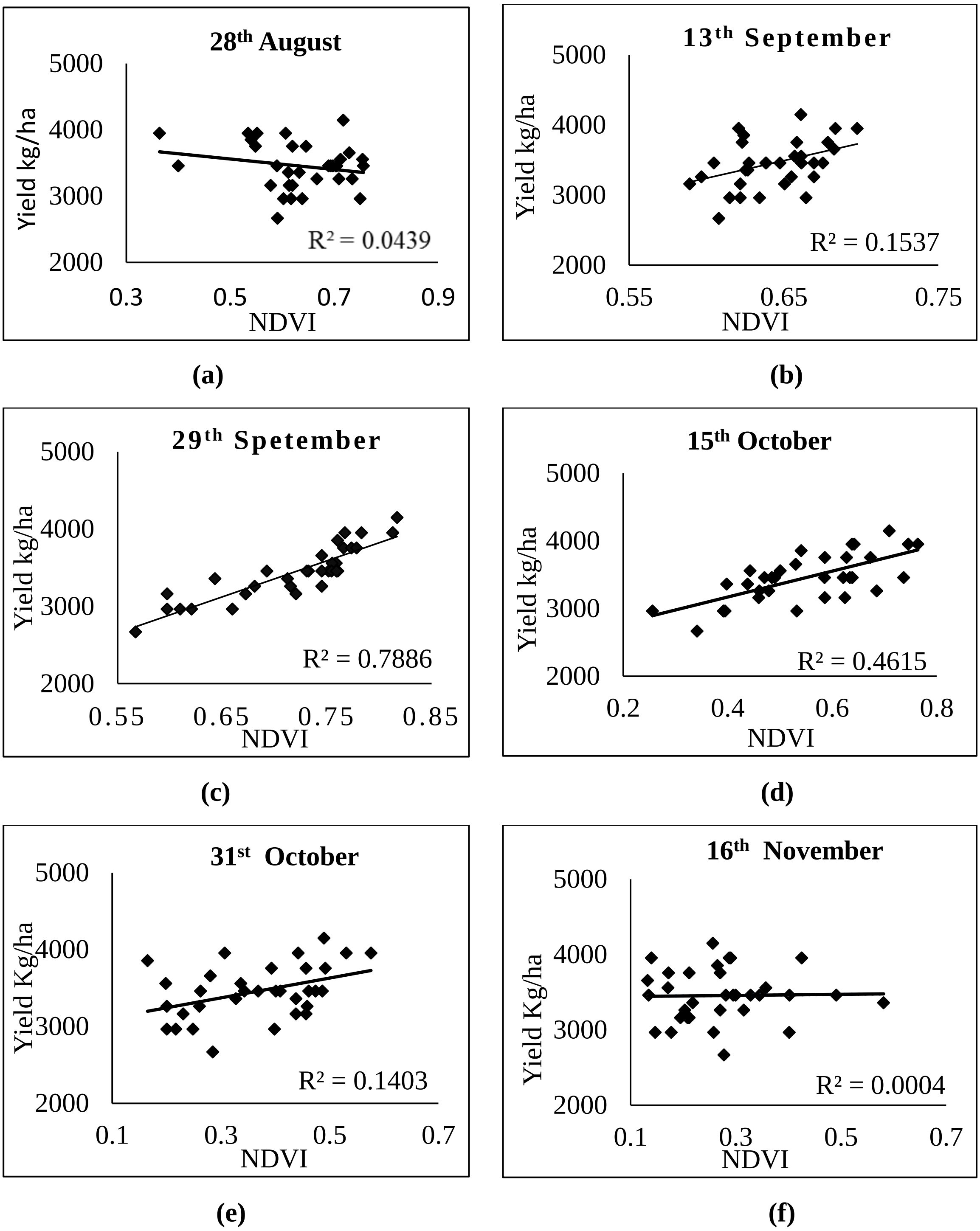

Figure 4.5. Linear regression curve showing relationship between Four Pixels (FP) Mean NDVI values and Observed rice yield of 33 sites on: (a) 28thAugust (b) 13th September (c) 29th September (d) 15thOctober (e) 31st October (f) 16th November.

yield started increasing up-to the month of September (13 September R^2= 0.1537; 29th September R^2= 0.7886) because of the increase in biomass. However it declined in October (15th October R^2= 0.4615; 31st October R^2= 0.1403) and November (R^2= 0.0004) due to the decreasing chlorophyll content in the leaves (Figure 4.2) The relationship observed in Figure 4.5c (29 September 2015) was used in forecasting the Rice yield with the following equation:

$$\mathrm{Y} = (419.57 \text{ x } 29 \text{ September NDVI}) - 8.2655 \quad \text{....................................Equation 4.1}$$

4.2 Mean NDVI and R^2 Values of NP & FP for All Surveyed Site

A comparison of mean NDVI and R2 values of all the 33 sites for six imagery was done to identify the highest values of the nine-pixel window. The imagery taken on 29th September showed the highest mean NDVI as well as the R2 values (NDVI= 0.7166; R2 = 0.5548) of all (Table 4.1). Likewise, a comparison of mean NDVI and R2 values for four pixels windows of all the 33 sites conformed the same conclusions regarding the imagery of 29th September (NDVI = 0.7212; R2 = 0.7886). The values of NDVI and R2 for four pixel window were higher than those of nine pixel window (Table 4.2) thereby, indicating the accuracy and reliability of the methodology used.

4.3 Validation of the Process for Determining Relationship between NDVI Values and Crop Yield

For validation of the process to determine the highest relationship between mean NDVI values and the observed yield, a graph was plotted showing values of R^2 and NDVI of all imageries against the time scale of imageries (Figure 4.6). NDVI values vary as the crop undergoes physiological changes and increases in biomass till maturity. In the early growing stages, the biomass of plants gradually increased giving higher values of NDVI corresponding to the increased in biomass.

Table 4.1. Mean NDVI of 33 sites and their R^2 values for nine Pixels

Sr. No	Date Of acquisition	Mean NDVI of Selected site	R^2 of nine Pixels mean NDVI and Observe Yield
1	28-Aug-2015	0.624279266	0.0214
2	13-Sep-2015	0.630484044	0.1256
3	29-Sep-2015	0.716582276	0.5548
4	15-Oct-2015	0.556842279	0.3563
5	31-Oct-2015	0.382805003	0.0902
6	16-Nov-2015	0.289776657	0.0105

Table 4.2. Mean NDVI values of 33 sites and their R^2 values for four Pixels

Sr. No	Date Of acquisition	Mean NDVI of Selected site	R^2 of four Pixels mean NDVI and Observe Yield
1	28-Aug-2015	0.633986758	0.0439
2	13-Sep-2015	0.6427995	0.1537
3	29-Sep-2015	0.721155659	0.7886
4	15-Oct-2015	0.549136038	0.4615
5	31-Oct-2015	0.364533773	0.1403
6	16-Nov-2015	0.273730508	0.0004

The peak NDVI value was observed on 29th of September, which indicated the crop maturity. It, was followed by plant senesces resulting in reduction in NDVI values. Likewise, the R2 values too underwent changes reaching their peak on 29th September (R^2=0.788; $p \leq 0.05$). The graph (Figure 4.6) showed that the peaks of the R^2 and NDVI curves coincided on the timeline of 29th September. This amply proved the reliability and validity of the process followed.

4.4 The Correlation between Observed and Calculated Yields

RS-based yield for all the 33 sites of four pixel window was calculated using regression equation (Equation 4.1) based on the NDVI values of 29th September imagery. The calculated yield was then compared with the observed yield and the variation between the two values was determined. The variation in the values of two yields was between -16% & +8 % (Appendix 2). The calculated yield was regressed against the observed yield to evaluate their relationship. The results showed a very significant relationship (R2 = 0.7383; $p \leq 0.05$) between the observed yield and RS-based calculated yield (Figure 4.7).

4.5 The Calculation of Area and Total Production of Sheikhupura

The total area and production under rice cultivation was calculated, came out to be 189496.35 hectares and 389559 tons respectively. The results were compared with the data provided by the Crop Reporting Survey of Punjab and the calculated production and cropped area was found to be 14.6% and 9% higher than the reported values respectively (Table 4.3)

4.6 Calculated & Observed Rice Yield Map Generation

A classified map of calculated yield was generated. The map showed three representative colors indicating variation in yield per pixels. The ranges included low vegetation with 200-300 kg/pixel, medium vegetation ranging from 301-380 kg/pixel and high vegetation having 381-500 kg/pixel (Figure 4.8).

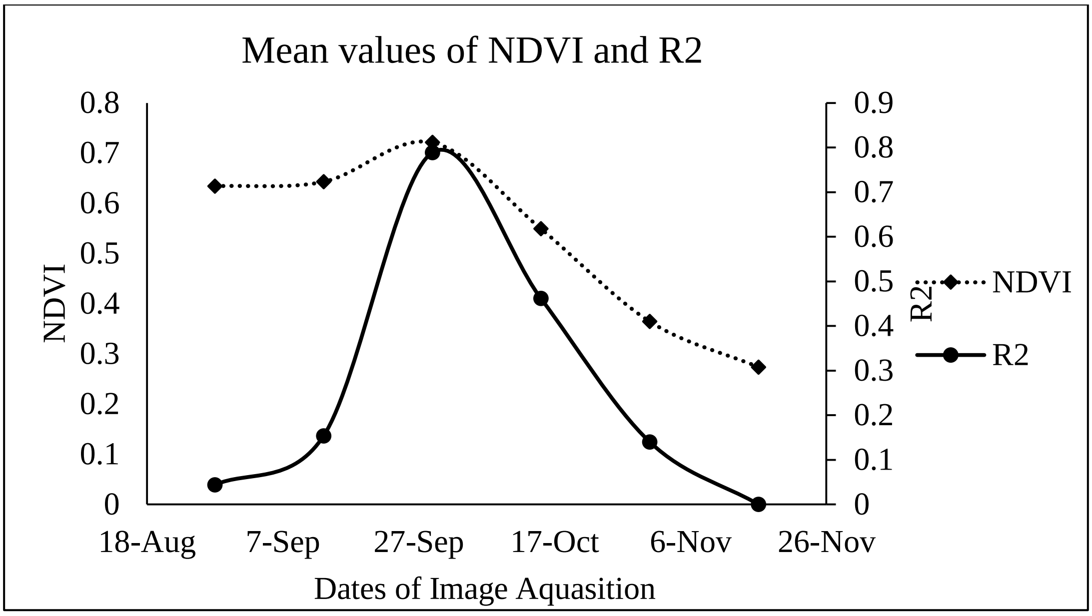

Figure 4.6. Graph showing relationship of NDVI and R^2 (four pixels methodology).

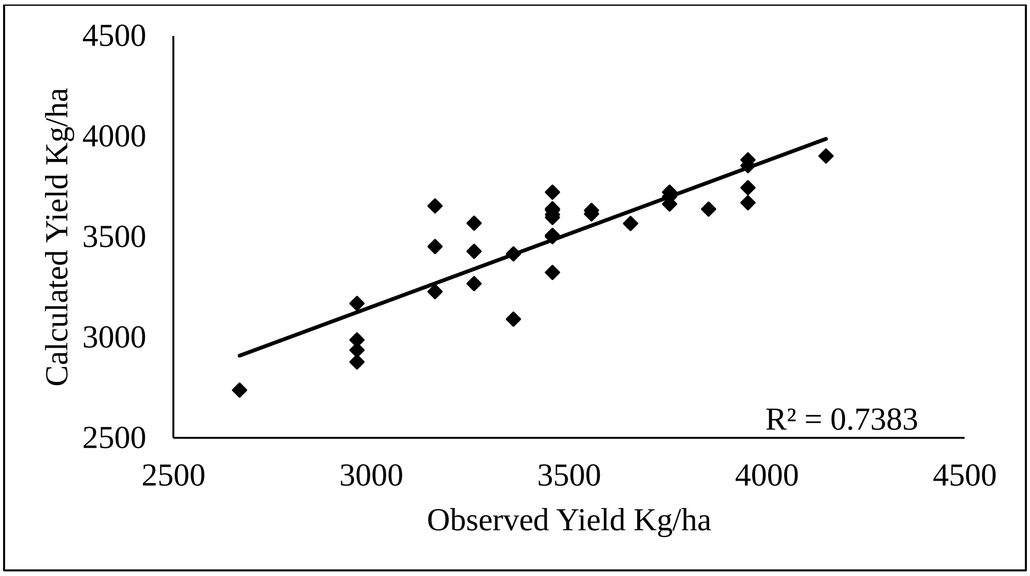

Figure 4.7. Relationship between observed and calculated yields

Table 4.3. Comparison of the Calculated and Reported cultivated Area, production of rice and their Percentage Variation.

Year	Calculated (Prod: In '000' Tonnes)	Reported (Prod: In '000' Tonnes)	Production Variation (%)	Calculated (Area In '000' Hectares)	Reported (Area In '000' Hectares)	Area Variation (%)
2015-16	389.559	332.50	+14.6%	189.496	172.39	+9%
2014-15		356.58	+15%		200.31	-5%

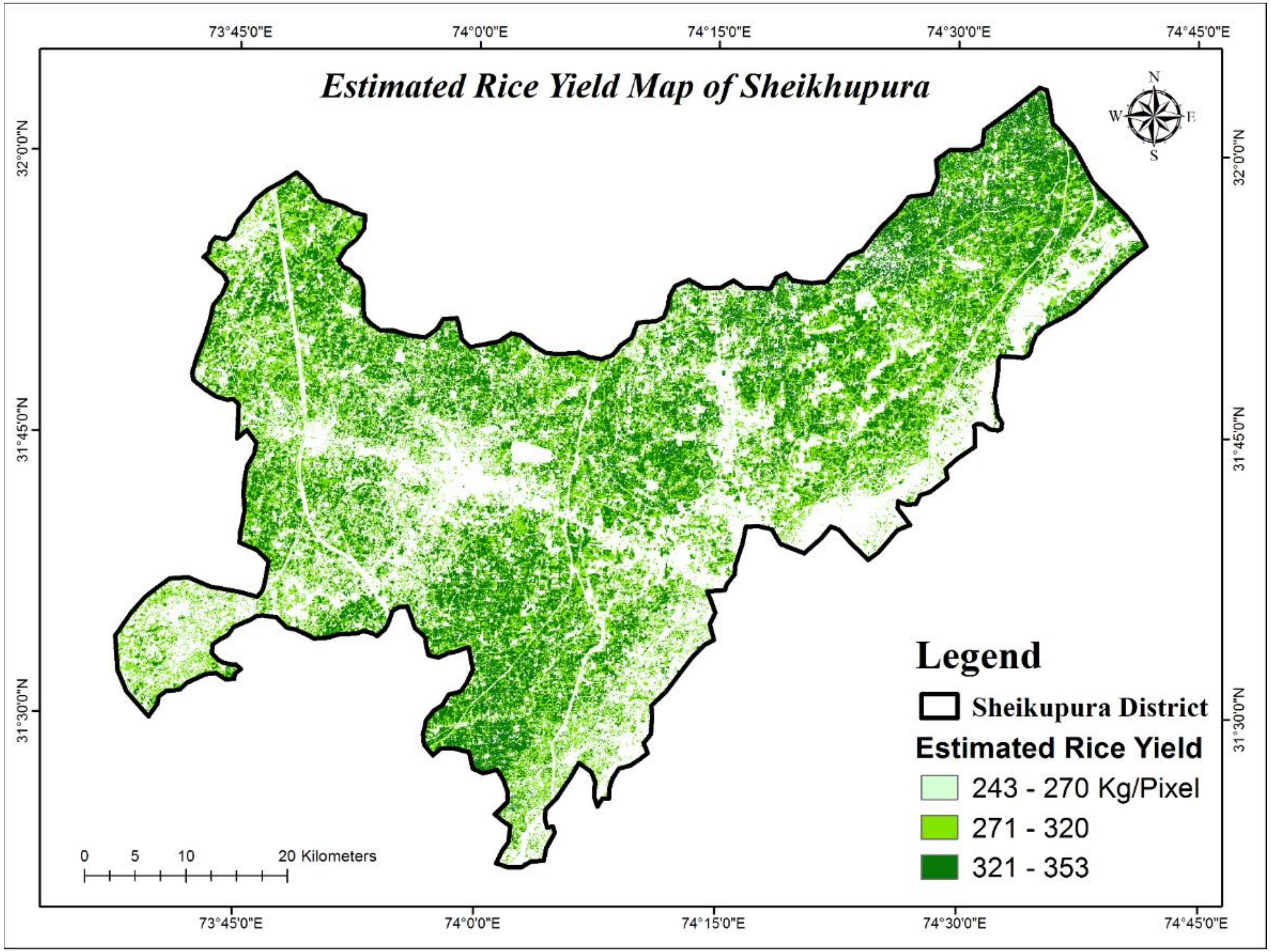

Figure 4.8. Calculated rice yield map of Sheikhupura.

For the sake of comparison and improving the reliability of results, an interpolated map observed yield was also generated in Arc GIS (Figure 4.9). The variation between the values of yields of two maps (1.25% to 5%) was found to be within the variation limits.

4.7 DSSAT-CSM Based Yield Forecasting

Appendix 3 gives the difference in observed and simulated yields and their percentage variation. The variation between the observed and simulated yields was between -3% to +10%. Figure 4.9 showed the regression curve between observed and simulated yields, where the value of R^2 was 0.93, which meant that the values of two yields have a high correlation between them.

4.8 Calculated and Simulated Rice Yields Comparison

Appendix 4 gives the percentage difference between simulated and calculated yields. The variation in the two yields ranges between -14% and + 6%, which is within acceptable limits. An RMSE of 178 and R^2 value of 0.738 ($p \leq 0.05$) was found between observed and NDVI estimated yield (Figure 4.10). On the other hand an RMSE of 111 and R^2 value of 0.928 ($p \leq 0.05$) was observed between actual yield and DSSAT simulated yield (Table 4.4). The results of the study showed that the DSSAT-CSM predicted the rice grain yield more accurately than the RS technique. However, DSSAT-CSM needs extensive data input and has constraints of spatial extrapolation.

4.9 Discussion

The results showed that the DSSAT-CSM predicted the grain yield more accurately than the Remote sensing-based technique as represented by the validation skills score for both (Table 4.3). The closer look at the skill score showed that the CSM produced better results than the RS. The study also revealed that both DSSAT-CSM and RS-based techniques had limitations

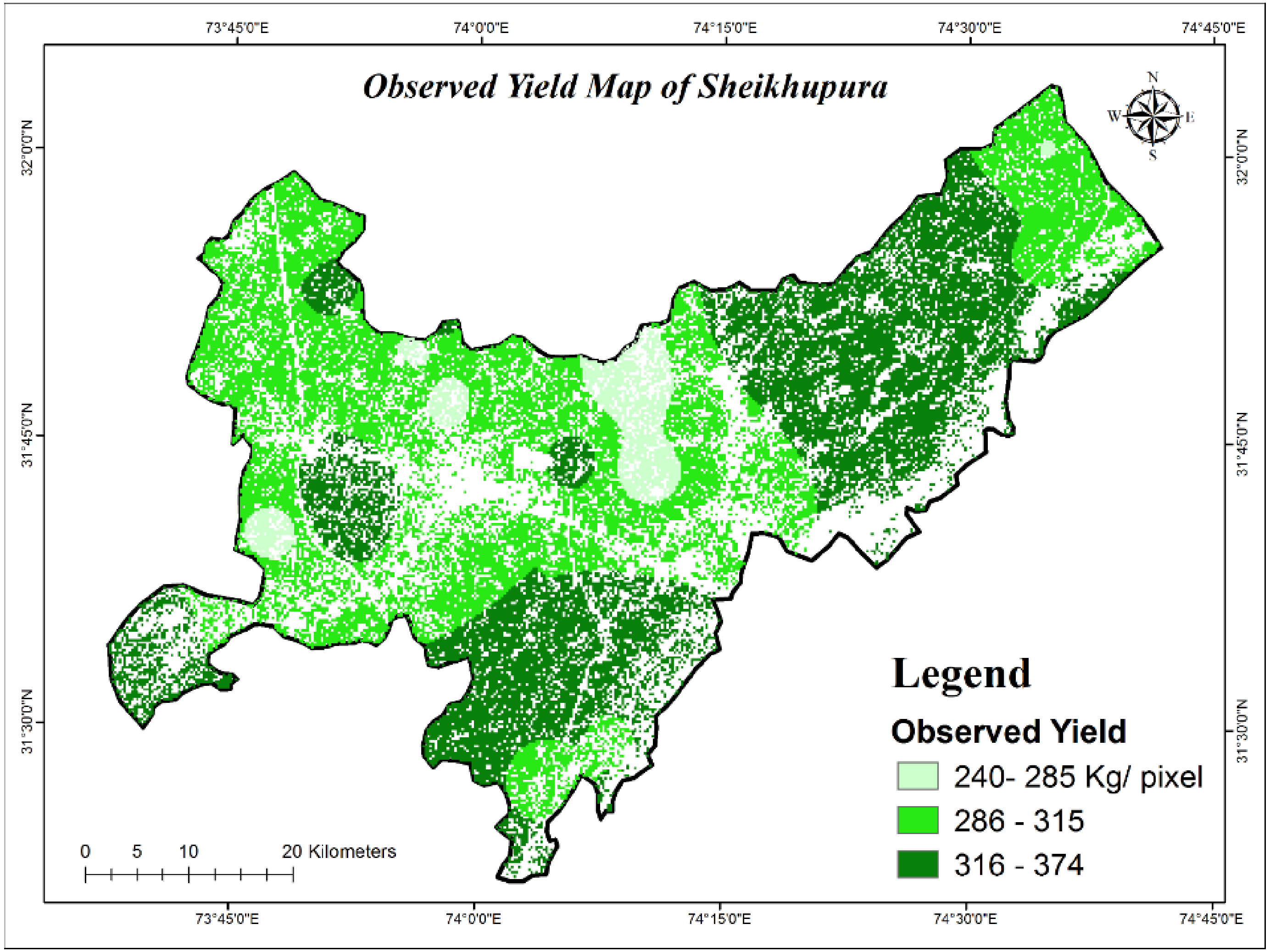

Figure 4.9. Rice crop observed yield map of Sheikhupura.

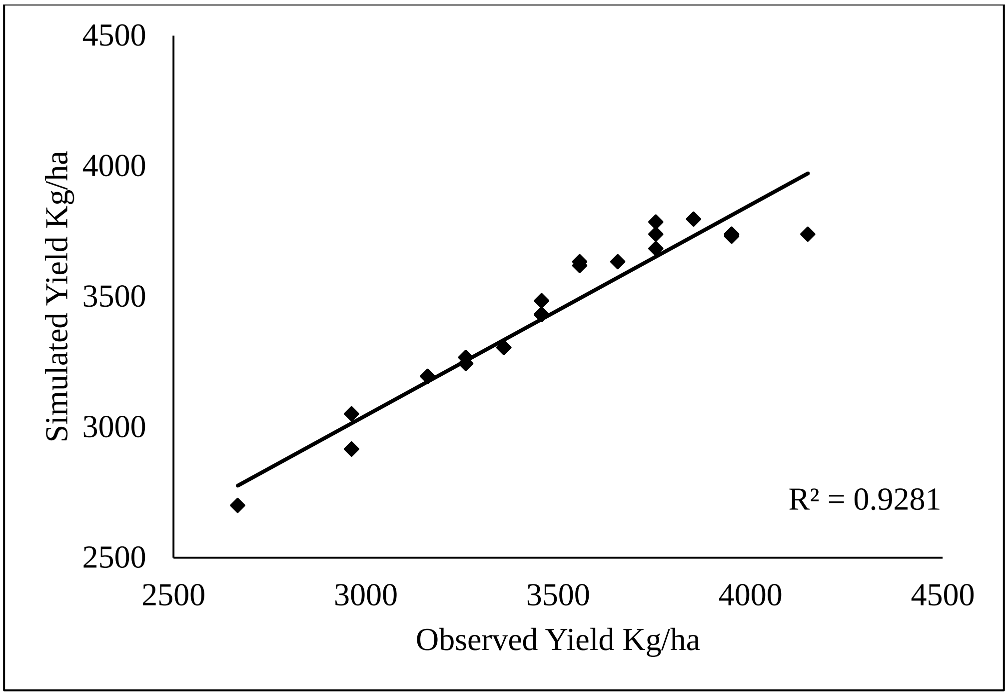

Figure 4.10. Showing relationship between observed and simulated rice grain yield.

Table 4.4. Statistical comparison of crop model and remote sensing based yield.

Method	**RMSE**	**R^2**
DSSAT-CSM	111.08	0.92
Remote sensing	178.76	0.73

that could be overcome if the two approaches are used to complement each other and the additional technologies are introduced to supplement then. DSSAT-CSM requires excessive data inputs for greater accuracy, but its application is confined to the areas whose complete input data is fed to the model. It has a limitation in spatial extrapolation, and thereby the calculation of crop production for larger area becomes very difficult by using the model alone. It however does help to assess future risks to the crop yield because of the climate change. Remote Sensing is an effective tool for predicting crop yields over a larger area through extrapolation. Landsat image has lesser resolution and is therefore not as effective as the SPOT satellite but has the advantage of covering the larger area. The Landsat has three basic limitations: (1) lesser spatial resolution, that impacts the accuracy in identifying the desired crop area and hence the calculation of total production taking into account variance in the derived results (2) sensitivity to weather conditions especially cloud coverage, smog/fog etc. that impacts the image quality and consequently the prediction of yield (3) has low temporal resolution (i.e., 16 days) that restricts the analysis to the days of satellites visits and (4) swath coverage (i.e., approximately 180 km). These limitations can be overcome by supplementing Landsat imagery by the use of drones over the target area and calibration of the selected sites using hand held spectrometer etc.

Chapter 5

CONCLUSIONS & RECOMMENDATIONS

5.1 Conclusion

This research work focused on the comparison of crop modelling with remote sensing and field survey. Field survey was used for extensive mapping of the research area and collection of rice crop management data from the farmers. An effort was thus made to apply RS & GIS technologies to agriculture management thereby promoting inter-disciplinary research and finding solution to the in-season forecasting of yield of crops. The research methodology, analysis of materials, application of relevant research tools and results of the research have amply demonstrated that:-

- A combination of rice yield forecasting by RS & GIS, DSSAT- CSM and field survey is possible and quite effective. However, it requires intensive efforts to collect extensive data, and that too under severe time constraints. Nonetheless, the outcomes justify the means and the methods used to complete the project.
- Remote sensing technique was used successfully to forecast the rice yield / production at the regional scale. However the level of accuracy for rice yield forecasting using Landsat 8 was affected by its low resolution, spatial variability within the scene and the negative effect of cloud cover during the crop growing season.
- The DSSAT-CERES model was successfully validated for simulating the rice yield. The results showed that DSSAT-CSM is an effective tool for accurate forecasting of rice yield. Since it needs extensive data input and accurate calibration, it gives more accurate results than those by RS. However, DSSAT-CSM has spatial constraints and would need additional data to extend its spatial application.

5.2 Recommendations

This research effort has laid a solid foundation for further inter-disciplinary research and application of technology to agriculture sector for its transition to informed decision making at the policy level. Timely rice yield forecasting is very helpful in planning rice exports while ensuring that country's food reserves are adequate to meet the domestic requirement. Following is recommended for follow-up research and studies:-

- Yield forecasting using remote sensing may be improved using multispectral images with high resolution (like SPOT imagery etc) to determine the specific rice signature.
- Multi-date and multi-radar imagery could be used for rice area mapping to offset the adverse impact of cloud coverage on the quality of remotely sensed imagery.
- The application of this research approach may be extended to other areas as well to increase its application in crop management.
- Field survey needs more deliberate planning especially when extensive data has to be collected for RS as well as DSSAT-CSM. It means that the conventional field survey techniques have to be complimented by imagery collected through drones. The supplementary use of instruments like handheld spectrometer would help to calibrate remote sensing and DSSAT-CM models, and improve crop management.
- The use of remote sensing imagery for live data input to DSSAT-CSM is now being tried at a number of places. This would help to combine the strengths of the two techniques and offset their limitations to a great extent. It is however an expensive option and needs a dedicated organization with requisite skills and resources to undertake the exercise on continuous basis. In Pakistan, agriculture extension department will have to be revamped to implement this option for meaningful results.

REFERENCES

1. Agrawal, A., Raskar, R., Nayar, S. K., & Li, Y. (2005). Removing photography artifacts using gradient projection and flash-exposure sampling. ACM Transactions on Graphics (TOG), 24(3), 828-835.
2. Ahmad, I., Ghafoor, A., Bhatti, M. I., & Akhtar, I. U. H. (2014). Satellite Remote Sensing and GIS based Crops Forecasting & Estimation System in Pakistan. Crop monitoring for improved food security.
3. Akhtar, W., Sharif, M., & Akmal, N. (2007). Analysis of economic Efficiency and Competitiveness of the Rice Production Systems of Pakistan's Punjab.
4. Al-Gaadi, K. A. (2010). Remote sensing, geographic information system and modeling techniques for wheat area and production estimation. Karnataka Journal of Agricultural Sciences, 23(4).
5. Amjad, R. (2010). Key Challenges Facing Pakistan Agriculture: How Best Can Policy Makers Respond? A Note: Islamabad: Pakistan Institute of Development Economics (PIDE).
6. Aparicio, N., Villegas, D., Casadesus, J., Araus, J. L., & Royo, C. (2000). Spectral vegetation indices as nondestructive tools for determining durum wheat yield. Agronomy Journal, 92(1), 83-91.
7. Ashraf, M. A., Maah, M. J., & Yusoff, I. (2011). Introduction to Remote Sensing of Biomass. doi:10.5772/16462
8. Baret, F., & Guyot, G. (1991). Potentials and limits of vegetation indices for LAI and APAR assessment. Remote sensing of environment, 35(2-3), 161-173.
9. Basso, B., Cammarano, D., & Carfagna, E. (2013, July). Review of crop yield forecasting methods and early warning systems. In Proceedings of the First Meeting of the Scientific Advisory Committee of the Global Strategy to Improve Agricultural and Rural Statistics, FAO Headquarters, Rome, Italy (pp. 18-19).
10. Briscoe, J., & Qamar, U. Pakistan's water economy : running dry. (44375), 1-155. Retrieved from http://documents.worldbank.org/curated/en/2005/11/9596145/pakistans-water-economy-running-dry
11. Campbell, J. B., & Wynne, R. H. (2011). Introduction to remote sensing. Guilford Press.

12. Cooley, T., Anderson, G., Felde, G., Hoke, M., Ratkowski, A., Chetwynd, J., Berk, A. (2002). FLAASH, a MODTRAN4-based atmospheric correction algorithm, its application and validation. Paper presented at the Geoscience and Remote Sensing Symposium, 2002. IGARSS'02. 2002 IEEE International.
13. Kamthonkiat, D., Honda, K., Turral, H., Tripathi, N., & Wuwongse, V. (2005). Discrimination of irrigated and rainfed rice in a tropical agricultural system using SPOT VEGETATION NDVI and rainfall data. International Journal of Remote Sensing, 26(12), 2527-2547.
14. Daughtry, C., Gallo, K., Goward, S., Prince, S., & Kustas, W. (1992). Spectral estimates of absorbed radiation and phytomass production in corn and soybean canopies. Remote sensing of environment, 39(2), 141-152.
15. Dempewolf, J., Adusei, B., Becker-Reshef, I., Hansen, M., Potapov, P., Khan, A., & Barker, B. (2014). Wheat yield forecasting for Punjab Province from vegetation index time series and historic crop statistics. Remote Sensing, 6(10), 9653-9675.
16. Fang, H. (1998). Rice crop area estimation of an administrative division in China using remote sensing data. International Journal of Remote Sensing, 19(17), 3411-3419.
17. Frouin, R., & Pinker, R. T. (1995). Estimating photosynthetically active radiation (PAR) at the earth's surface from satellite observations. Remote sensing of environment, 51(1), 98-107.
18. Hoogenboom, G., Jones, J., Wilkens, P., Porter, C., Batchelor, W., Hunt, L., . . . Bowen, W. (2004). Decision support system for agrotechnology transfer version 4.0. University of Hawaii, Honolulu, HI (CD-ROM).
19. Gallo, K., Daughtry, C., & Bauer, M. E. (1985). Spectral estimation of absorbed photosynthetically active radiation in corn canopies. Remote sensing of environment, 17(3), 221-232.
20. Garbulsky, M. F., Peñuelas, J., Gamon, J., Inoue, Y., & Filella, I. (2011). The photochemical reflectance index (PRI) and the remote sensing of leaf, canopy and ecosystem radiation use efficiencies: A review and meta-analysis. Remote sensing of environment, 115(2), 281-297.
21. Gausman, H. (1973). Reflectance, transmittance, and absorptance of light by subcellular particles of spinach (Spinacia oleracea L.) leaves. Agronomy Journal, 65(4), 551-553.
22. Gausman, H., & Allen, W. (1973). Optical parameters of leaves of 30 plant species. Plant Physiology, 52(1), 57-62.

23. Gausman, H., Allen, W., Cardenas, R., & Richardson, A. (1971). Effects of Leaf Nodal Position on Absorption and Scattering Coefficients and Infinite Reflectance of Cotton Leaves, Gossypium hirsutum L. Agronomy Journal, 63(1), 87-91.
24. Gausman, H., Allen, W., & Escobar, D. (1974). Refractive index of plant cell walls. Applied Optics, 13(1), 109-111.
25. Gausman, H., Allen, W., Myers, V., & Cardenas, R. (1969). Reflectance and Internal Structure of Cotton Leaves, Gossypium hirsutum L. Agronomy Journal, 61(3), 374-376.
26. Gausman, H., Gerbermann, A., Wiegand, C., Leamer, R., Rodriguez, R., & Noriega, J. (1975). Reflectance differences between crop residues and bare soils. Soil Science Society of America Journal, 39(4), 752-755.
27. Gausman, H., & Hart, W. (1974). Reflectance of sooty mold fungus on citrus leaves over the 2.5 to 40-micrometer wavelength interval. Journal of Economic Entomology, 67(4), 479-480.
28. GeoHive. (2010). Historic, current and future population: Asia. Retrieved from http://www.geohive.com/earth/his_proj_asia.aspx
29. Holm, A., Burnside, D., & Mitchell, A. (1987). The development of a system for monitoring trend in range condition in the arid shrublands of Western Australia. The Rangeland Journal, 9(1), 14-20.
30. Hoogenboom, G. (2000). Contribution of agrometeorology to the simulation of crop production and its applications. Agricultural and Forest Meteorology, 103(1), 137-157.
31. Pachauri, R. K., Allen, M. R., Barros, V., Broome, J., Cramer, W., Christ, R., Dasgupta, P. (2014). Climate change 2014: synthesis Report. Contribution of working groups I, II and III to the fifth assessment report of the intergovernmental panel on climate change: IPCC.
32. Jame, Y., & Cutforth, H. (1996). Crop growth models for decision support systems. Canadian Journal of Plant Science, 76(1), 9-19.
33. Jones, J. W., Hoogenboom, G., Porter, C. H., Boote, K. J., Batchelor, W. D., Hunt, L., Ritchie, J. T. (2003). The DSSAT cropping system model. European Journal of Agronomy, 18(3), 235-265.
34. Khush, G. S. (2005). What it will take to feed 5.0 billion rice consumers in 2030. Plant molecular biology, 59(1), 1-6.
35. Kirthiga, S. (2013). Regional Crop Yield Forecast by Integrated Use of Climate & Crop Models with aid of RS and GIS Techniques. Indian Space Research Organization.

36. Matthew, M. W., Adler-Golden, S. M., Berk, A., Felde, G., Anderson, G. P., Gorodetzky, D., . . . Shippert, M. (2002). Atmospheric correction of spectral imagery: evaluation of the FLAASH algorithm with AVIRIS data. Paper presented at the Applied Imagery Pattern Recognition Workshop, 2002. Proceedings. 31st.
37. McCloy, K., Smith, F., & Robinson, M. (1987). Monitoring rice areas using Landsat MSS data. International Journal of Remote Sensing, 8(5), 741-749.
38. Mosleh, M. K., Hassan, Q. K., & Chowdhury, E. H. (2015). Application of remote sensors in mapping rice area and forecasting its production: A review. Sensors, 15(1), 769-791.
39. Mosleh, M. (2015). Use of GIS and Remote Sensing in Mapping Rice Areas and Forecasting Its Production at Large Geographical Extent. University of Calgary.
40. Motha, R. (2011). Use of Crop Models for Drought Analysis. Drought Mitigation Center Faculty Publications. Retrieved from http://digitalcommons.unl.edu/droughtfacpub/58.
41. Pakistan Economic Survey 2014-15, Ministary of finance, Islamabad, Pakistan. Retrieved from http://www.finance.gov.pk/survey_1415.html.
42. Pakistan Economic Survey 2015-16, Ministary of finance, Islamabad, Pakistan. Retrieved from http://www.finance.gov.pk/survey_1415.html.
43. Noureldin, N. ., Aboelghar, M. ., Saudy, H. ., & Ali, A. . (2013) Rice yield forecasting models using satellite imagery in Egypt. The Egyptian Journal of Remote Sensing and Space Science, 16(1), 125–131.
44. Prasad, A., Singh, R., Tare, V., & Kafatos, M. (2007). Use of vegetation index and meteorological parameters for the prediction of crop yield in India. International Journal of Remote Sensing, 28(23), 5207-5235.
45. Reyniers, M., Vrindts, E., & De Baerdemaeker, J. (2004). Fine-scaled optical detection of nitrogen stress in grain crops. Optical Engineering, 43(12), 3119-3129.
46. Roderick, M., Smith, R., & Lodwick, G. (1996). Calibrating long-term AVHRR-derived NDVI imagery. Remote sensing of environment, 58(1), 1-12.
47. Royo, C., Aparicio, N., Villegas, D., Casadesus, J., Monneveux, P., & Araus, J. (2003). Usefulness of spectral reflectance indices as durum wheat yield predictors under contrasting Mediterranean conditions. International Journal of Remote Sensing, 24(22), 4403-4419.
48. Sawasawa, H. L. (2003). Crop Yield Estimation: Integrating RS, GIS, and Management Factor. A case study of Birkoor and Kortigiri Mandals, Nizamabad District India, 1-9.

49. Sellers, P., Berry, J., Collatz, G., Field, C., & Hall, F. (1992). Canopy reflectance, photosynthesis, and transpiration. III. A reanalysis using improved leaf models and a new canopy integration scheme. Remote sensing of environment, 42(3), 187-216.
50. Serrano, L., Filella, I., & Penuelas, J. (2000). Remote sensing of biomass and yield of winter wheat under different nitrogen supplies. Crop Science, 40(3), 723-731.
51. Shanahan, J. F., Schepers, J. S., Francis, D. D., Varvel, G. E., Wilhelm, W. W., Tringe, J. M., . . . Major, D. J. (2001). Use of remote-sensing imagery to estimate corn grain yield. Agronomy Journal, 93(3), 583-589.
52. Siyal, A. A., Dempewolf, J., & Becker-Reshef, I. (2015). Rice yield estimation using Landsat ETM+ Data. Journal of Applied Remote Sensing, 9(1), 095986-095986.
53. Solari, F., Shanahan, J., Ferguson, R., Schepers, J., & Gitelson, A. (2008). Active sensor reflectance measurements of corn nitrogen status and yield potential. Agronomy Journal, 100(3), 571-579.
54. Tucker, C., & Sellers, P. (1986). Satellite remote sensing of primary production. International Journal of Remote Sensing, 7(11), 1395-1416.
55. Wheeler, T., & Von Braun, J. (2013). Climate change impacts on global food security. Science, 341(6145), 508-513
56. Wiegand, C. L., & Richardson, A. J. (1990). Use of spectral vegetation indices to infer leaf area, evapotranspiration and yield: I. Rationale. Agronomy Journal, 82(3), 623-629.
57. Shiu, Y.-S., Lin, M.-L., Huang, C.-H., & Chu, T.-H. (2012). Mapping paddy rice agriculture in a highly fragmented area using a geographic information system object-based post classification process. Journal of Applied Remote Sensing, 6(1), 063526-063521-063526-063515.
58. 11th Five Year Plan 2013-18 Planning commission, Ministry of planning, Development and Reform Islamabad. (2013). Islamabad, Pakistan.

APPENDICES

Appendix 1 Field survey data of rice crop in Sheikhupura

Sr. No	LAT	LONG	Name of Farmer	Address of Farm visited Village,UC, Tehsil
1	31.57833	73.76444	Ahmad Saeed	Allah ditta Koat, Bahawal Koat, Sheikhupura
2	31.66889	73.79417	Zafar Iqbal	Makki 460, 84 Makki 460/Butter, Sheikhupura
3	31.74861	73.78111	Asghar Ali	Bhedan Ala Dera, Kot Sondha 82 Sheikhupura
4	31.72194	73.71722	M. Anwar	Sawan ky Shamola Dera dabea, Bhali ky, Safdrabad
5	31.68167	73.67333	Zia Ullah Cheema	Mitto Tibi, Jhandian wala, Safdrabad
6	31.66444	74.98108	Nasir Hussain	Jaitta, Barianwala, Shekhupur
7	31.81417	74.22693	Ameer Ali	Bhatian ala, Khothiala, Muredky
8	31.76583	74.22526	Khalid Javed	Chak 34, noon 16, Muredky
9	31.72778	74.16839	Asif Sultan	Vandala Nasir Khan, Bhianala, Muredky
10	31.84	73.73833	M. Nawaz	Chambal, Rachand, Shekhupur
12	31.78167	73.74343	M. Iqbal	Rachand, Rachand 79, Shekhupur
13	31.79556	73.77767	Asim Mahboob	Thatha Bahadur Shah, Rachand 79 Sheikhupura
14	31.88111	73.84132	Haji Abdullah	Dera Kerra , chabran, Sheikhupura
15	31.82306	73.9342	M. Asif	Jandiala sher khan, peer waris shah 72, Sheikhupura
16	31.84861	73.95955	M. Aslam	Mashmola Derra bhaat Wala/ Madaar Dera bhathan Maddar, Shekhupur
17	31.7825	73.97156	Jabbar Ali	Mirza Virkan, Mirza virkan, Shekhupur
18	31.80667	73.92605	M. Awais Akram	Jandiala sher khan, peer waris shah 72, Sheikhupura
19	31.90806	73.81351	Asghar Ali	Kelly, Kakar gill/Kelly, Sheikhupura
20	31.87111	73.75715	Amjad Ali	Borh Bath, Kakar gill, Sheikhupura

21	31.46679	74.07833	M. Arif	Metha tarida, Koat Mahmood, Sharaqpur
22	31.52066	74.09888	Rehmat Ali	Kaviabad, Sharaqpur/marapangwan, Sharaqpur
23	31.56848	74.10673	Chaman Abbas	Kishanpur, 22 Chak, Sharaqpur
24	31.56136	74.18	M. Tofail	Morraa ala, Morra ala, Ferozwala
25	31.49694	74.13972	Riasat Ali	Lurky nemat, Mandianwala, Sharaqpur
26	31.77993	74.02014	Muzamil Ijaz	Chachoky, Mirzan virkan, Sheikhupura
27	31.73229	74.0988	Mian Tehseen Jabbar	Kherpur Malian, Malian kalaan, Muredky
28	31.80544	74.1646	Naseer Ahmad	kothiala virkan, Malian kallan, Muredky
29	31.84488	74.29627	Amjad Shah	kothiala virkan, Malian kallan, Muredky
30	31.88336	74.40989	M. Aslam	Jutt Chehl, Lambery, Muredky
32	31.9145	74.48092	Shahid Mahmood	Chak Butty/ Derra Yaqoob, Kitto Sharif, Muredky
33	31.91219	74.56316	Nasir Mahmood	Kot bhilan, Narang mandi, Muredky

Area Under Rice Cultivation	Rice Seed Variety	DAP/bags/ Acre	Urea bags /acre	Irrigation	Previous cro	Time of Sowing	Time of Harvesting	Observed Yield 2015
9	PS2	2.5	2	Flood	Wheat	15-Jul	15-Oct	3458
7	PS2	1	0	Flood	Wheat	18-Jul	25-Oct	2964
9	PS2	0	1	Flood	Wheat	15-Jul	30-Oct	3162
13	PS2	1	1	Flood	Wheat	12-Jul	15-Oct	3952
26	PS2	1	1	Flood	Wheat	15-Jul	20-Jan	3754
12	PS2	1	1	Flood	Wheat	03-Jul	18-Oct	3260
8	PS2	1	1	Flood	Wheat	03-Jul	20-Oct	3458
25	PS2	1	1	Flood	Wheat	30-Jun	22-Oct	3260
36	PS2	0	0	Flood	Wheat	21-Jun	18-Oct	2964
10	PS2	0	0	Flood	Wheat	22-Jun	13-Oct	3458
150	PS2	0	1	Flood	Wheat	30-Jul	01-Nov	3359
52	PS2	1	1	Flood	Wheat	23-Jul	05-Nov	3162
22	PS2	1	1	Flood	Wheat	18-Jul	04-Nov	3754
20	PS2	0	0	Flood	Wheat	23-Jun	14-Oct	2964
2.5	PS2	2	2	Flood	Wheat	07-Jul	22-Oct	3557
40	PS2	0	0	Flood	Wheat	30-Jul	25-Oct	2964
20	PS2	1	1	Flood	Wheat	16-Jul	04-Nov	3458
40	PS2	1	1	Flood	Wheat	22-Jul	10-Nov	3260
8	PS2	1	2	Flood	Wheat	19-Jul	03-Nov	3359

48	PS2	1	2	Flood	Wheat	15-Jul	30-Oct	3458
25	PS2	2	2	Flood	Wheat	13-Jul	26-Oct	3557
5	PS2	1	1	Flood	Wheat	21-Jul	02-Nov	3853
30	PS2	0	0	Flood	Wheat	24-Jul	05-Nov	3754
65	PS2	1	1	Flood	Wheat	20-Jul	08-Nov	3458
20	ps2	0	0	flood	wheat	17-Jul	08-Nov	3458
140	PS2	0	0	Flood	Wheat	20-Jul	29-Oct	3656
13	PS2	0	0	Flood	Wheat	19-Jun	12-Oct	2668
14	PS2	1	1	Flood	Wheat	19-Jul	02-Nov	4150
200	PS2	1	1	Flood	Wheat	20-Jul	01-Nov	3952
1	PS2	1	1	Flood	Wheat	18-Jul	05-Nov	3952
20	PS2	1	1	Flood	Wheat	25-Jul	25-Oct	3458
40	PS2	1	1	Flood	Wheat	26-Jul	27-Oct	3952
15	PS2	1	1	Flood	Wheat	24-Jul	02-Nov	3162

Appendix 2 Calculated and Observed Yield and their % difference.

Sr. No	Latitude	Longitude	Observed Yield kg/ha (Yo)	Calculated Yield Kg/ha Yc	Difference Yo-Yc	% Difference Yo-Yc/Yo*100
1	31.57833	73.76444	3458	3597	-139	-4
2	31.66889	73.79417	2964	3169	-205	-7
3	31.74861	73.78111	3162	3451	-290	-9
4	31.72194	73.71722	3952	3744	208	5
5	31.68167	73.67333	3754	3663	91	2
6	31.66444	74.98108	3260	3567	-306	-9
7	31.81417	74.22693	3458	3722	-264	-8
8	31.76583	74.22526	3260	3268	-7	0
9	31.72778	74.16839	2964	2936	28	1
10	31.84	73.73833	3458	3322	136	4
11	31.78167	73.74343	3359	3090	269	8
12	31.79556	73.77767	3162	3227	-65	-2
13	31.88111	73.84132	3754	3699	56	1
14	31.82306	73.9342	2964	2878	86	3
15	31.84861	73.95955	3557	3631	-74	-2
16	31.7825	73.97156	2964	2987	-23	-1
17	31.80667	73.92605	3458	3507	-49	-1
18	31.90806	73.81351	3260	3427	-167	-5
19	31.87111	73.75715	3359	3414	-55	-2
20	31.46679	74.07833	3458	3639	-181	-5

21	31.52066	74.09888	3557	3613	-56	-2
22	31.56848	74.10673	3853	3637	216	6
23	31.56136	74.18	3754	3722	33	1
24	31.49694	74.13972	3458	3610	-152	-4
25	31.77993	74.02014	3458	3500	-42	-1
26	31.73229	74.0988	3656	3566	89	2
27	31.80544	74.1646	2668	2737	-70	-3
28	31.84488	74.29627	4150	3902	248	6
29	31.88336	74.40989	3952	3883	69	2
30	31.9145	74.48092	3952	3855	97	2
31	31.91219	74.56316	3458	3633	-175	-5
32	31.54918	73.6501	3952	3670	282	7
33	32.00654	74.58062	3162	3653	-491	-16

Appendix 3 Simulated and Observed Yield and their % differences.

Sr. No	Latitude	Longitude	Observed Yield kg/ha (Yo)	Simulated Yield Kg/ha (Ys)	Difference (Yo-Ys)	% Difference Yo-Ys/Yo* 100
1	31.57833	73.76444	3458	3483	-25	-1
2	31.66889	73.79417	2964	2915	49	2
3	31.74861	73.78111	3162	3194	-32	-1
4	31.72194	73.71722	3952	3739	213	5
5	31.68167	73.67333	3754	3739	15	0
6	31.66444	74.98108	3260	3243	17	1
7	31.81417	74.22693	3458	3483	-25	-1
8	31.76583	74.22526	3260	3267	-7	0
9	31.72778	74.16839	2964	3050	-86	-3
10	31.84	73.73833	3458	3431	27	1
11	31.78167	73.74343	3359	3305	54	2
12	31.79556	73.77767	3162	3194	-32	-1
13	31.88111	73.84132	3754	3683	71	2
14	31.82306	73.9342	2964	2915	49	2
15	31.84861	73.95955	3557	3618	-61	-2
16	31.7825	73.97156	2964	2915	49	2
17	31.80667	73.92605	3458	3431	27	1
18	31.90806	73.81351	3260	3267	-7	0
19	31.87111	73.75715	3359	3305	54	2
20	31.46679	74.07833	3458	3431	27	1

21	31.52066	74.09888	3557	3633	-76	-2
22	31.56848	74.10673	3853	3796	57	1
23	31.56136	74.18	3754	3785	-31	-1
24	31.49694	74.13972	3458	3431	27	1
25	31.77993	74.02014	3458	3431	27	1
26	31.73229	74.0988	3656	3633	23	1
27	31.80544	74.1646	2668	2699	-31	-1
28	31.84488	74.29627	4150	3739	411	10
29	31.88336	74.40989	3952	3731	221	6
30	31.9145	74.48092	3952	3731	221	6
31	31.91219	74.56316	3458	3431	27	1
32	31.54918	73.6501	3952	3739	213	5
33	32.00654	74.58062	3162	3194	-32	-1

Appendix 4 Simulated and Calculated Yields and their percentage difference

Sr. No	Latitude	Longitude	Simulated Yield kg/ha (Ys)	Calculated Yield Kg/ha (Yc)	Difference (Ys-Yc)	% Difference Ys-Yc/Yo*100
1	31.57833	73.76444	3483	3597	-114	-3
2	31.66889	73.79417	2915	3169	-254	-9
3	31.74861	73.78111	3194	3451	-257	-8
4	31.72194	73.71722	3739	3744	-5	0
5	31.68167	73.67333	3739	3663	76	2
6	31.66444	74.98108	3243	3567	-324	-10
7	31.81417	74.22693	3483	3722	-239	-7
8	31.76583	74.22526	3267	3268	-1	0
9	31.72778	74.16839	3050	2936	114	4
10	31.84	73.73833	3431	3322	109	3
11	31.78167	73.74343	3305	3090	215	6
12	31.79556	73.77767	3194	3227	-33	-1
13	31.88111	73.84132	3683	3699	-16	0
14	31.82306	73.9342	2915	2878	37	1
15	31.84861	73.95955	3618	3631	-13	0
16	31.7825	73.97156	2915	2987	-72	-2
17	31.80667	73.92605	3431	3507	-76	-2
18	31.90806	73.81351	3267	3427	-160	-5
19	31.87111	73.75715	3305	3414	-109	-3
20	31.46679	74.07833	3431	3639	-208	-6
21	31.52066	74.09888	3633	3613	20	1

22	31.56848	74.10673	3796	3637	159	4
23	31.56136	74.18	3785	3722	63	2
24	31.49694	74.13972	3431	3610	-179	-5
25	31.77993	74.02014	3431	3500	-69	-2
26	31.73229	74.0988	3633	3566	67	2
27	31.80544	74.1646	2699	2737	-38	-1
28	31.84488	74.29627	3739	3902	-163	-4
29	31.88336	74.40989	3731	3883	-152	-4
30	31.9145	74.48092	3731	3855	-124	-3
31	31.91219	74.56316	3431	3633	-202	-6
32	31.54918	73.6501	3739	3670	69	2
33	32.00654	74.58062	3194	3653	-459	-14